Title	Studies on Construction of Functional Wrinkles at Hydrogel Interfaces
Author(s)	加藤, 雅俊
Citation	大阪大学, 2020, 博士論文
Version Type	VoR
URL	https://doi.org/10.18910/76520
rights	
Note	

Doctoral Dissertation

Studies on Construction of Functional Wrinkles at Hydrogel Interfaces

（ハイドロゲル界面における機能性リンクルの構築に関する研究）

Masatoshi Kato

January 2020

Graduate School of Engineering,

Osaka University

Contents

General Introduction

The surfaces of materials is one of the most important parts because it always comes in contact with other materials or environments. The geometrical configuration of surface plays a key role in energy or material exchange. In nature, many micro- and/or nano-sized 3-D structures such as holes,[1,2] scales[3] and cilia[4-7] are often observed. These 3-D structures act to increase the surface area of material. Finger prints,[8,9] gecko-feet,[10] moth antennas[11] and butterfly wings[2] have acquired specific functions due to the increased surface area and their micro- and/or nano-sized structures. Due to their unique functions, the geometrical configuration of materials are focused. Inspired by these attractive features, many researchers have attempted to mimic their topologies. In fact, fabrication methods of unique surfaces with specific functions such as dry adhesives,[6, 12] super hydrophobicity,[13] anti-reflection[14] and structure colors[15, 16] have been reported. Therefore, bioinspiration is one of the ways to fabricate highly functionalized materials using their surface morphology.

Among the above-described microstructures, wrinkles are ones of the most easily generated structures at the elastic material surface. Wrinkle structures are formed by buckling of elastic material surface due to the surface instability. They are usually described as two-layered structures in which hard-thin films are laminated on the surface of elastic substrate. Wrinkles were fabricated on the surface of many kinds of materials such as substrate (gels[17], elastomers[18] and thermoplastics[19]) using external stimulus to cause surface instability (mechanical stretching[20], heating[21], swelling[22], *etc.*) with hard thin layer structures (bilayer[23] and gradient[24]). Therefore, wrinkle structures would be easily fabricated at surface and/or interface of materials. The wavelength (λ) of wrinkle structures are described by the following equation (**eq. 1**).[25,26]

$$\lambda = 2\pi t\left(\frac{E_\mathrm{f}}{3E_\mathrm{s}}\right)^{1/3} \qquad \textbf{(eq. 1)}$$

where, t is the thickness of thin film, and E_f and E_s are the Young's moduli of the thin film and elastic substrate. Thus, the wavelength of wrinkles is easily controlled by the modulus of elastic substrate and/or hard thin layer thickness. Wrinkle structures were also found in nature, and they were formed at the surface and interface of biological tissues such as brains, fingers,[8] and flowers.[27] It is considered that these wrinkle structures at the surface of biological tissues play a role of increasing the material surface, but the functions of some wrinkle structures at the surface of biological tissue are still unclear. Because of the interesting shape and the function of increasing the surface area, the creation method of wrinkles and surface functionalization using wrinkles have been vigorously investigated. In fact, functional materials such as ultra-sensitive pressure sensor[28] and smart window[29] were developed using the increased surface area and the wrinkled geometries. In these materials, wrinkle structures occupy an important place for increasing the interaction between wrinkled surface and external environments. Usually, these wrinkle structures are formed by hard thin layer fabrication using surface oxidation[12] and micro-sized metal particle spattering[15] on the surface of elastic materials (**Fig. 1**). These methods are usually performed for pre-stretched or pre-swelled elastomers such as poly(dimethylsiloxane).

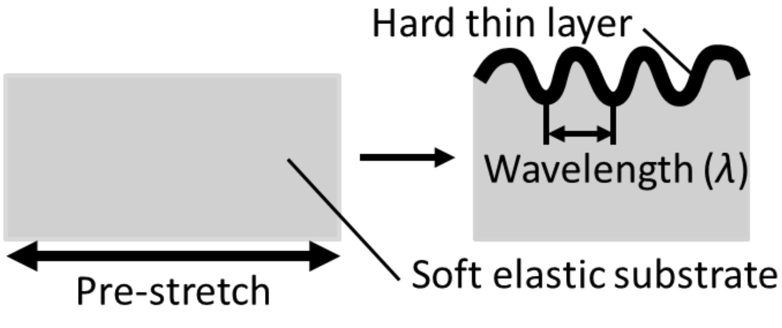

Fig. 1. Illustration of wrinkle fabrication by formation of hard thin layer on the elastic substrate.

However, as described above, wrinkle structures in nature are formed at the surface of biological tissues which contains many amount of water. The present hard layer fabrication methods for elastomer are not suitable for water containing materials. Therefore, novel wrinkle fabrication method in water environment is required for elucidation of their functions in living tissues and/or fabrication of the mimicking materials using surface wrinkles.

Hydrogel is one of elastic materials and consists of hydrophilic polymer, cross-linking points and water (**Fig. 2**). Hydrogels are prepared from many kinds of basis materials (hydrophilic polymers/monomers, polysaccharides, gelatin, *etc*.) and cross-linking ways (chemical and physical crosslinking, gamma-ray irradiation *etc*.). Presently, hydrogels are applied to disposable diapers, contact lenses, and anti-vibration hydrogels. The mechanical and chemical properties of hydrogels can be widely changed by control their polymer network structures. For examples, double-network hydrogels,[30] topological gels,[31] and tetra-armed polyethyleneglycol hydrogels[32] show a great property in tensile strength, elongation, and modulus due to their spatial networks. Because of their hydrophilicity and biocompatibility, hydrogels are expected as a next-generation materials such as artificial tissues[33] and drug-delivery system.[34] Functionalization of hydrogels is easily carried out by using copolymerization, side-chain reaction and introduction of other materials into their polymer networks. Their many functions are

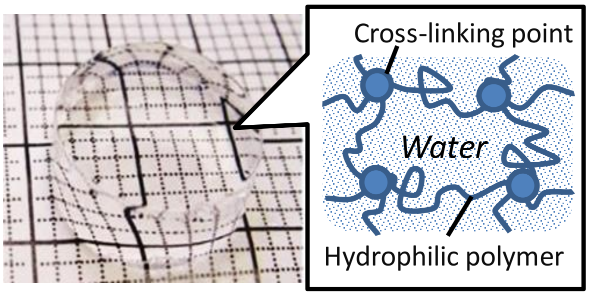

Fig. 2. Image and schematic illustration of hydrogels.

performed at or through their surface (**Table 1**). [35-40] Thus, novel functions are expected by formation of wrinkle structures at the surface of hydrogels. Actually, fabrication of micro-sized multi cellular spheroids are achieved using the wrinkle structure at the surface of hydrogels.[41] Nowadays, wrinkle fabrication methods for hydrogels were studied by swelling around their surface[42], grafting stimuli-responsive polymers[43] and formation of hybrid-silica layer.[44] In these methods, origins of wrinkle formation are swelling around surface of hydrogels and/or fabrication of crust layer at the surface of hydrogels. However, these methods require special pre-arrangements for hydrogels or techniques to create the instability around hydrogel surface. Thus, a novel easy post fabrication method of surface wrinkle structures for hydrogel is required.

Table 1. Functions and applications using gels.

Functions	Applications	Ref.
Separation	Chromatography	35
Molecular sensing	Sensors	36
Light sensing	Smart windows, Light sensors, Displays	37
Reaction control	Micro reactors, Enzyme recovery	38
Molecular inclusion	Drug delivery, Drug carrier	34
Cell control	Cell culture sheet	39
Shape memory	Medical supplies	40

In this thesis, the author focused on a polyion complex (PIC), which was formed by mixing cationic and anionic polymers in aqueous solutions, and was easily prepared on the surface of hydrogels.[45,46] It is well-known that thin-layered PICs were prepared using layer-by-layer (LbL) method.[47] Generally, LbL method is a cyclic process in which a charged polymer is adsorbed onto a substrate, and after washing, an oppositely charged polymer is adsorbed on top of the first layer. This constitutes a single bi-layer with a thickness generally on the order of nanometers, and the deposition process can be repeated until a multilayer film of desired thickness has been assembled.[48] Their moduli were reported to be several hundred MPa in water.[49] This means the Young's moduli of PIC layer is much higher than that of hydrogels (~100 kPa). Therefore, the author hypothesized that the formation of wrinkle structures would be achieved by the fabrication of PIC at the surface of hydrogels using electrophoresis.

Moreover, stimuli-responsive polymers are also focused due to their character of being controllability by external stimulus. Represented stimuli-responsive polymers in water are shown in **Fig. 3**.[50-52] By using such stimuli-responsive polymers, stimuli-responsive hydrogels which can change their property by external stimulus, are prepared. In particular, some kinds of hydrogels change their Young's modulus triggered by coil-

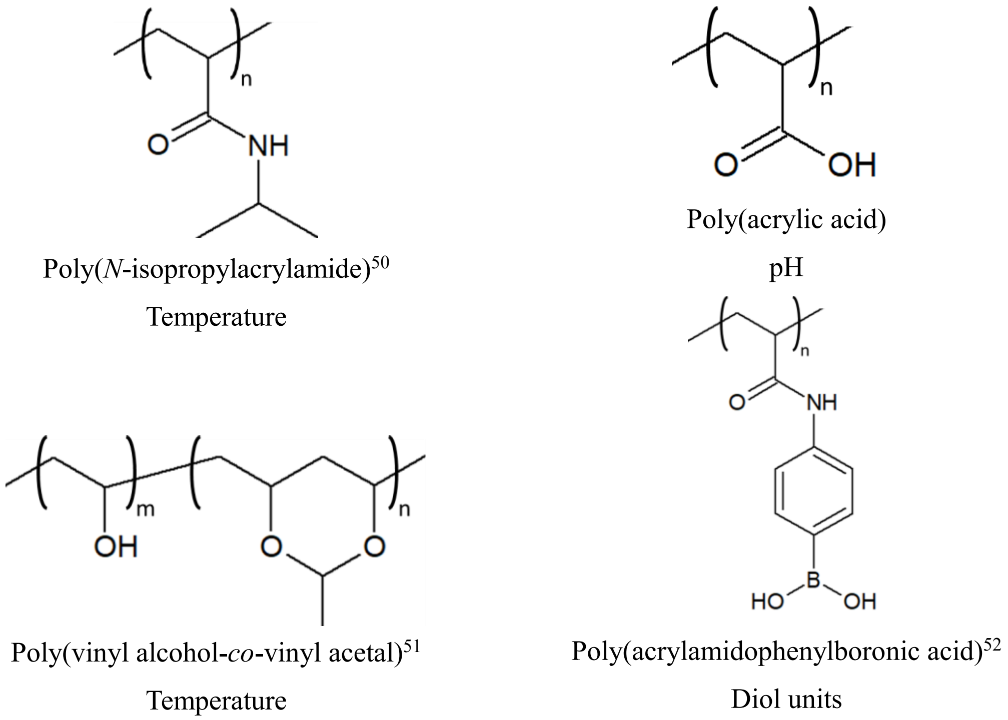

Poly(*N*-isopropylacrylamide)[50]
Temperature

Poly(acrylic acid)
pH

Poly(vinyl alcohol-*co*-vinyl acetal)[51]
Temperature

Poly(acrylamidophenylboronic acid)[52]
Diol units

Fig. 3. Stimuli-responsive polymers and their external stimuli in water.

globule phase transition, in response to external stimuli. It means that the instability between hard skin layer and soft hydrogels as substrate would be changed by using stimuli-responsive hydrogels. Thus, the wrinkle formed by the stress-instability between hard thin film and soft substrate should be switched by using stimuli-responsive materials. If the geometrical configurations of wrinkle structures were switched by the changing of surface instability, the wavelength and amplitude of wrinkle structures should be also changed. In fact, stimuli-responsive wrinkles were fabricated at the surface of polycaprolactones elastomers.[53] The substrate can control its function for alignment of cells using stimuli-responsive wrinkle structures. Therefore, stimuli-responsive wrinkle structure at the hydrogel surface would control the functions of wrinkled surface by external stimuli. Stimuli-responsive wrinkled hydrogel surfaces would be a new platform to use water containing materials.

In this doctoral thesis, fabrication methods of functional wrinkles for hydrogel and their ability at the interfaces of hydrogels were focused. This thesis is composed of 3 chapters.

In Chapter 1, a novel wrinkle formation method for hydrogel surface in aqueous condition was developed using electrophoresis (**Fig. 4**). In this method, wrinkle structures were induced by the Young’s modulus mismatch between polyion complex (PIC) layer

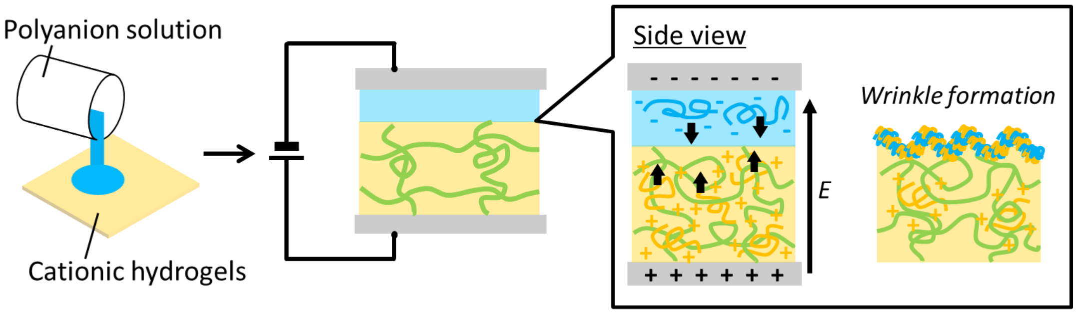

Fig. 4. Schematic illustration of electrophoretic wrinkle fabrication method.

formed at the hydrogel surface by electrophoresis, and hydrogel as a soft substrate. The wavelength of wrinkle structures was easily controlled by electrophoresis condition and Young's modulus of hydrogel. Preparation of patterned and gradient wrinkles was possible by modulating the electrode insulation. Aligned wrinkles was fabricated at the surface of uniaxially stretched hydrogels. The geometry pattern of aligned wrinkles were changed by Young's modulus of hydrogels and stretching ratio during electrophoresis. After unloading, hierarchical wrinkle structures were fabricated at the surface of highly stretched hydrogels. Creation of active wrinkle structures which can switch their geometrical configuration were achieved using thermoresponsive hydrogels as substrate.

In Chapter 2, wrinkle structures at gel-gel interface were fabricated by PIC layer formation at their adhered interface using electrophoresis (**Fig. 5**). The key factor of wrinkle formation was investigated by spatial control of polymer network of hydrogels, including the density, distribution, and interactive units. Wrinkle structures were fabricated at the adhered interface of hydrogels which have semi-interpenetrated polymer networks (semi-IPNs) structure. The role of wrinkle structures at the interface of hydrogels in adhesion was investigated by the measurement of adhesive strength and

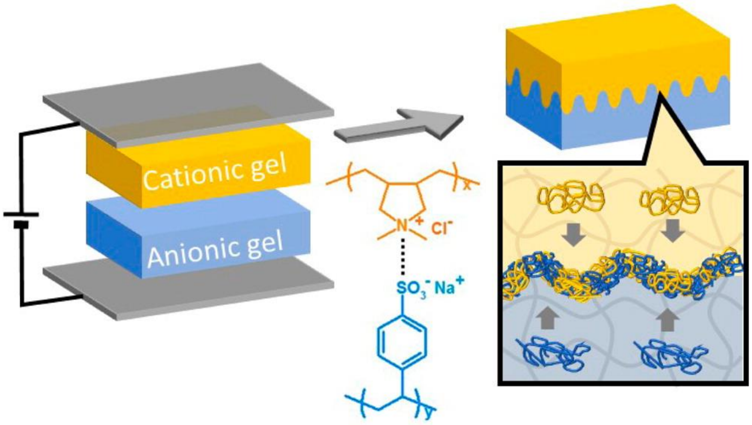

Fig. 5. Schematic illustration of wrinkle structure formation at the interface of adhered hydrogels.

observation of interface structures of hydrogels which adhered under compression stress. As a result, wrinkle formation was inhibited and the adhered strength of hydrogels was decreased by compression of hydrogels during electrophoresis. Thus, it was founded that wrinkles at the interface of hydrogels have a function to increase the adhesive strength of hydrogels.

In Chapter 3, a novel adhesion method for hydrogels was developed using swelling-induced wrinkling films (**Fig. 6**). Two pieces of hydrogels was adhered by sandwiching a dried gel film. The interface structures such as flat, creased and wrinkled were controlled by the swelling ratio of wrinkling films. The role of wrinkle formation was investigated by adhesive strength of hydrogels. Aligned wrinkles were formed with anisotropic swelling gel-films. The adhesive strength of hydrogels with wrinkles parallel to tensile direction was larger than that of perpendicular wrinkles. Adhered gels were easily detached by peeling of wrinkled hydrogel film. Moreover, thermoresponsive

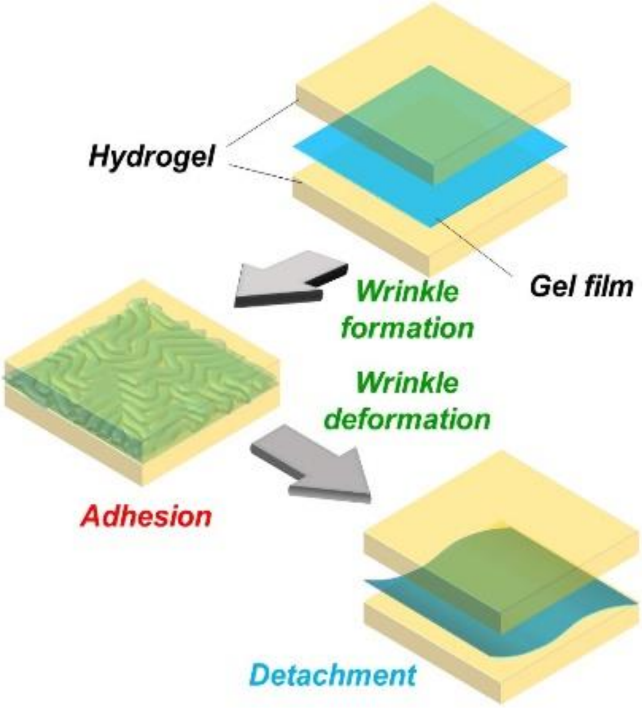

Fig. 6. Illustration of adhesion control of hydrogels using wrinkled hydrogel film.

hydrogel film was used to control the wrinkle structure at the interface of adhered hydrogels by temperature. The adhered interface was stable in cold water because of the existence of wrinkles at the interface of wrinkles; however, they detached in hot water due to wrinkle deformation triggered by temperature change. By using wrinkles at the adhered interface of hydrogels, both strong adhesion and easy detachment were achieved.

In this thesis, the author proposed the wrinkle formation method utilizing the interface instabilities of hydrogels. Wrinkle structures were fabricated by simple and easy methods utilizing interface instabilities. Using stimuli-responsive hydrogels, the interface instability was changed, and wrinkle shapes were switched by modulus changing of gels triggered by external stimuli. The function of wrinkles were also switched using stimuli-responsive wrinkles. Such highly functionalized wrinkles can control their functions, and they will be able to use for new applications as functional hydrogel surfaces.

References

1. F. Noll, M. Sumper, N. Hampp. *Nano Lett.* **2002**, *2*, 91-95.
2. S. U. Cho, D. I. Kim, W. K. Cho, B. S. Shin, M. Y. Jeong. *ACS Appl. Mater. Interfaces* **2016**, *8*, 29770-29778.
3. H. Tada, S. E. Mann, I. N. Miaoulis, P. Y. Wong. *Appl. Opt.* **1998**, *37*, 1579-1584.
4. Z. L. Wu, R. Wei, A. Buguin, J. M. Taulemesse, N. L. Moigne, A. Bergeret, X. Wang, P. Keller. *ACS Appl. Mater. Interfaces* **2013**, *5*, 7485-7491.
5. H. Shahsavan, B. Zhao. *Soft Matter* **2012**, *8*, 8281-8284.
6. G. Castellanos, E. Arzt, M. Kamperman. *Langmuir* **2011**, *27*, 7752-7759.
7. Y. Maeno, Y. Nakayama. *Appl. Phys. Lett.* **2009**, *94*, 012103.
8. K. Kareklas, D. Nettle, T. V. Smulders. *Biol. Lett.* **2013**, *9*, 20120999.
9. M. Kücken, A. C. Newell. *J. Theor. Biol.* **2005**, *235*, 71-83.
10. K. Autumn, Y. A. Liang, S. T. Hsieh, W. Zesch, W. P. Chan, T. W. Kenny, R. Fearing. R. J. Full. *Nature* **2000**, *405*, 681-685.
11. B. S. Hansson, H. Ljungberg, E. Hallberg, C. Löfstedt. *Science* **1992**, *256*, 1313-1315.
12. E. P. Chan, E. J. Smith, R. C. Hayward, A. J. Crosby. *Adv. Mater.* **2008**, *20*, 711-716.
13. Y. Li, S. Dai, J. John, K. R. Carter. *ACS Appl. Mater. Interfaces* **2013**, *5*, 11066-11073.
14. K. Nagashima, A. Kosuge, Y. Ochi, M. Tanaka. *Opt. Express* **2013**, *16*, 18640-18645.
15. A. E. Schedl, C. Neuber, A. Fery, H. W. Schmidt. *Langmuir* **2018**, *34*, 14249-14253.
16. E. Tian, Y. Ma, L. Cui, J. Wang, Y. Song, L. Jiang *Macromol. Rapid Commun.* **2009**, *30*, 1719-1724.
17. M. Leocmach, M. Nespoulous, S. Manneville, T. Gibaud. *Sci. Adv.* **2015**, *1*, 1500608.
18. X. Cheng, L. Miao, Z. Su, H. Chen, Y. Song, X. Chen, H. Zhang. *Microsys. Nanoeng.*

2017, *3*, 16074.

19. Y Zhao, W. Huang, Y. Fu. J. *Micromech. Microeng.* **2011**, *21*, 067007.
20. A. Auguste, L. Jin, Z. Suo, R. C. Hayward. *Soft Matter* **2014**, *10*, 6520-6529.
21. H. Hou, J. Yin, X. Jiang. *Adv. Mater.* **2016**, *28*, 9126-9132.
22. M. Guvendiren, S. Yang, J. A. Burdick. *Adv. Funct. Mater.* **2009**, *19*, 3038-3045.
23. Y. Chen, A. J. Crosby. *Adv. Mater.* **2014**, *26*, 5626-5631.
24. S. K. Basu, L.E. Scriven, L.F. Francis, A.V. McCormick. *Prog. Org. Coat.* **2005**, *53*, 1-16.
25. S. Yang, K. Khare, P. C. Lin. *Adv. Funct. Mater.* **2010**, *20*, 2550-2564.
26. A. L. Volynskii, S. Bazhenov, O. V. Lebedeva, N. F. Bakeev. *J. Mater. Sci.* **2000**, *35*, 547-554.
27. H. M. Whitney, M. Kolle, P. Andrew, L. Chittka, U. Steiner, B. J. Glover. *Science* **2009**, *323*, 130-133.
28. N. Gao, X. Zhang, S. Liao, H. Jia, Y. Wang. *ACS Macro Lett.* **2016**, *5*, 823-827.
29. G. Lin, P. Chandrasekaran, C. Lv, Q. Zhang, Y. Tang, L. Han, J. Yin. *ACS Appl. Mater. Interfaces* **2017**, *9*, 26510-26517.
30. J. P. Gong, Y. Katsuyama, T. Kurokawa, Y. Osada. *Adv. Mater.* **2003**, *15*, 1155-1158.
31. Y. Okumura, K. Ito. *Adv. Mater.* **2001**, *13*, 485-487.
32. T. Sakai, T. Matsunaga, Y. Yamamoto, C. Ito, R. Yoshida, S. Suzuki, N. Sasaki, M. Shibayama, U. Chung. *Macromolecules* **2008**, *41*, 5379-5384.
33. J. L. Drury, D. J. Mooney. *Biomaterials*, **2003**, *24*, 4337-4351.
34. T. R. Hoare, D. S. Kohane. *Polymer*, **2008**, *49*, 1993-2007.
35. K. Nagase, T. Okano. *J. Mater. Chem. B* **2016**, *4*, 6381-6397.
36. D. Buenger, F. Topuz, J. Groll. *Prog. Polym. Sci.* **2012**, *37*, 1678-1719.

37. R. Akashi, H. Tsutsui, A. Komura. *Adv. Mater.* **2002**, *14*, 1808-1811.
38. M. Miyazaki, H. Maeda. *Trends Biotechnol.* **2006**, *24*, 463-470.
39. K. Haraguchi, T. Takehisa, M. Ebato. *Biomacromolecules* **2006**, *7*, 3267-3275.
40. K. Matsumoto, A. Kawamura, T. Miyata. *Macromolecules* **2017**, *50*, 2136-2144.
41. Z. Zhao, J. Gu, Y. Zhao, Y. Guan, X. X. Zhu, Y. Zhang. *Biomacromolecules* **2014**, *15*, 3306-3312.
42. M. Ebara, K. Uto, N. Idota, J. M. Hoffman, T. Aoyagi. *Adv. Mater.* **2012**, *24*, 273-278.
43. M. Guvendiren, J. A. Burdick, S. Yang. *Soft Matter* **2010**, *6*, 2044-2049.
44. K. Matsukawa, T. Masuda, Y. S. Kim, A. M. Akimoto, R. Yoshida. *Langmuir* **2017**, *33*, 13828-13833.
45. Y. Takemoto, H. Ajiro, T. Asoh, M. Akashi. *Chem. Mater.* **2010**, *22*, 2923-2929.
46. H. Sakaguchi, T. Serizawa, M. Akashi. *Chem. Lett.* **2003**, *32*, 174-175.
47. J. J. Richardson, M. Björnmalm, F. Caruso. *Science* **2015**, *348*, aaa2491.
48. G. Decher. *Science* **1997**, *277*, 1232-1237.
49. B. Wu, C. Li, H. Yang, G. Liu, G. Zhang. *J. Phys. Chem. B* **2012**, *116*, 3106-3114.
50. Y. Hirokawa, T. Tanaka. *J. Chem. Phys.* **1984**, *81*, 6379.
51. D. Christova, S. Ivanova, G. Ivanova. *Polym. Bull.* **2003**, *50*, 367–372.
52. A. Matsumoto, T. Kurata, D. Shiino, K. Kataoka. *Macromolecules* **2004**, *37*, 1502-1510.
53. M. Ebara, K. Uto, N. Idota, J. M. Hoffman, T. Aoyagi. *Adv. Mater.* **2012**, *24*, 273-278.

Chapter 1.

Development of Novel Wrinkle Fabrication Method at Hydrogel Surfaces Using Electrophoresis

1.1 Introduction

Wrinkle structures are often observed around soft elastic interfaces such as fingers and brain in human body, and play an important role of gaining surface area. As a function of wrinkle structures, adsorption of micro-sized materials was studied.[1] Thus, it is expected that wrinkle structures at the surface of hydrogels show functions such as adsorption, adhesion and decreasing of light-reflection. As described above, wrinkle structures at the surface of hydrogel has a function such as spheroid formation.[2] In addition, stimuli-responsive wrinkles can switch the surface morphology and their functions. For example, the alignment of cells can be changed by the formation and deformation of wrinkle structures at the surface of elastic material.[3] Thus, if a stimuli-responsive wrinkle is fabricated at the hydrogel surface, the wrinkled hydrogels surface would be applied to control water-containing materials. Usually, wrinkle structures were fabricated by surface oxidation or metal sputtering for elastic material surfaces. However, conventional wrinkle formation methods are not suitable for hydrogels, due to mostly composed water. Hence, development of wrinkle fabrication method for hydrogels is required. Nowadays, wrinkle structures were fabricated by surface-localized polymer grafting[4] and hybrid silica layer modification.[5] In these studies, crust layers were fabricated at on the surface of hydrogels and the surface instability was caused by stress-mismatch. In this study, the author focused on polyion complex (PIC), which was formed by mixing cationic and anionic polymers in water[6,7] as surface hard thin layer. PIC has high Young's modulus (~200 MPa in water) comparing with hydrogels (~100 kPa). Thus, the author hypothesized that the wrinkle formation would be triggered by PIC fabrication at the surface of hydrogels.

In chapter 1, development of a novel wrinkle fabrication method using electrophoresis was achieved. The thin layer, composed of PIC on hydrogels was prepared by electrophoresis of polyanions in the direction of cationic hydrogels. To investigate the origin of wrinkle structure formation, the electrophoresis condition and the Young's modulus of hydrogels were changed. The patterned wrinkle and the gradient wrinkle were fabricated by modulating the electrodes. Moreover, aligned wrinkles was also fabricated at the surface of uniaxially stretched hydrogels. An active wrinkles which can switch their geometrical configuration, were prepared by using a thermoresponsive hydrogel.

1.2 Experimental Section

Materials.

N,N-Dimethylacrylamide (DMAAm) and *N*-isopropylacrylamide (NIPAAm) were purchased from FUJIFILM Wako Pure Chemical Corporation and used after distillation and recrystallization, respectively. *N,N*'-Methylenebisacrylamide (MBAAm) were purchased from FUJIFILM Wako Pure Chemical Corporation and used as purchased without further purification. Sodium poly(4-styrenesulfonate) (PSS), 4-stylenesulfonic acid sodium salt (SSNa), and fluorescein-*o*-acrylate were purchased from Aldrich and used as purchased without further purification. Poly(diallyldimethylammonium chloride) (PDDA) was purchased from Aldrich as aqueous solution and used after freeze dried. 2-Hydroxy-4'-(2-hydroxyethoxy)-2-methylpropiophenone (Irgacure 2959) was purchased from Tokyo Chemical Industry Co., Ltd. and used without further purification.

Preparation and characterization of cationic hydrogels.

Cationic DMAAm semi-interpenetrating network structure (semi-IPNs) hydrogels were prepared by free-radical polymerization of DMAAm (2.0 mol L^{-1}) with MBAAm (10 mmol L^{-1}) in the presence of PDDA using Irgacure 2959 (20 mmol L^{-1}) as photo-polymerization initiator (**Scheme 1-1**). All chemicals were dissolved into pure water and then the solution was degassed with sonication and aspiration. The concentration of charged group was fixed at 50 mmol L^{-1}. The degassed solution was poured into glass and silicon elastomer spacer mold. The specimen size was 90 x 90 x 1 mm^3. The intensity and irradiation time of UV light was 40 mW cm^{-2} at 365 nm and 40 min, respectively. The mold was flipped each 10 min. During polymerization, the

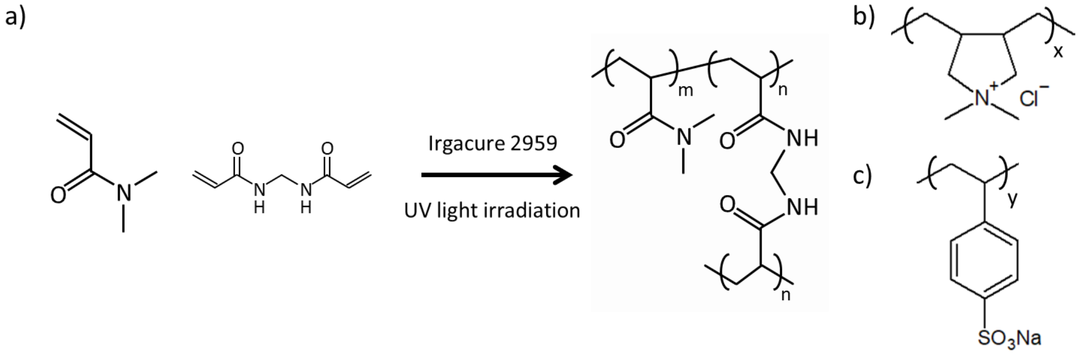

Scheme 1-1 (a) Preparation of PDMAAm hydrogel. (b, c) Chemical structures of (b) PDDA and (c) PSS.

temperature of pre-gel solution was kept at 4 °C. PNIPAAm hydrogels were prepared by free-radical polymerization of NIPAAm as monomer and other conditions were the same with the preparation of DMAAm gels. Prepared hydrogels were washed with water for the removal of unreacted monomer and initiator. Young's modulus of gels was measured by tensile test using tensile tester (Shimadzu EZ-Graph) in an ambient atmosphere. The tensile test was performed at 120 mm min^{-1} in tensile mode.

Formation of wrinkle structure on the hydrogel surface.

Wrinkle structures on the hydrogel surface were prepared by electrophoretic deposition of polymers (**Fig. 1-1**). 50 μL of aqueous PSS solution (50 mmol L^{-1} as ionic monomer units) was put on the top of cationic hydrogel and then they were sandwiched with two Pt electrodes. An electric field was applied to these sandwiched solution and hydrogel. After electrophoresis, hydrogels were washed with pure water.

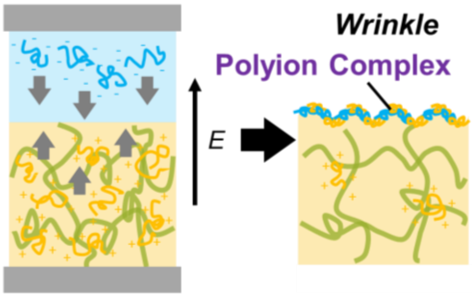

Fig. 1-1 Experimental procedure of wrinkle formation at hydrogel surface.

Formation of wrinkle structures at the surface of hydrogels under stretching.

Electrophoretic wrinkle fabrication method was performed under stretching. Aqueous PSS solution (50 μL) was put on the top of a stretched cationic hydrogel, then they were sandwiched with two pieces of Pt electrodes. An electric field (10 V mm^{-1}) was applied to these sandwiched solution and hydrogel. After electrophoresis, the surface was washed with pure water to remove excess PSS from hydrogel surface. The surface structure was observed by phase-contrast microscope (IX-73, Olympus) and white light coherence interferometer (VS-1330, HITACHI). Theremoresponsive-active wrinkles were prepared by same method using stretched PNIPAAm hydrogels.

Characterization of the wrinkle surface.

Fluoresce-labelled PSS (Flu-PSS) was prepared by copolymerization of SSNa and fluorescein-*o*-acrylate as fluorescence dye. Prepared Flu-PSS was purified by dialysis with regenerated cellulose dialysis membrane (Spectra/Por®, MWCO = 1 kD) to remove unreacted monomers. The Flu-PSS was used as anionic polymer for wrinkle formation process. The fluorescence microscopic observation was performed using an fluorescent microscope (IX-73, Olympus) with a 20x LUCPLFLN 0.45 NA objective, and the expose time was 50 ms. The U-HGLGPS high pressure mercury lamp was used for excitation.

1.3 Results and Discussion

After electrophoresis, hydrogels were optically transparent but wrinkle structures were observed by phase-contrast microscopic observation (**Fig. 1-2**). These wrinkle structures were not observed when an electric field was not applied in the absence of PSS. By impression of voltage, cationic PDDA and anionic PSS were moved to the cathode and the anode, respectively. Then, the PSS in the solution moved to the hydrogels surface that contains PDDA on anode side by electrophoresis. The PIC layer was formed on the hydrogel surface due to the electrostatic interaction between cationic PDDA and anionic PSS. After electrophoresis, the surface zeta potential value of hydrogel was changed from +10.8 mV to +0.48 mV, indicating that cationic hydrogel was covered with anionic PSS.

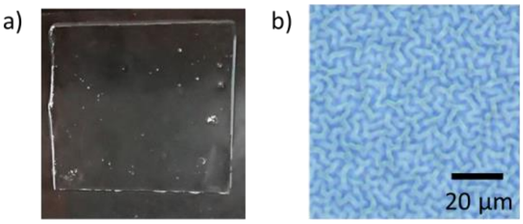

Fig. 1-2 (a) Macroscopic and (b) microscopic observations of wrinkled hydrogel surface.

Moreover, the fluorescence from the wrinkling surface with electrophoresis of Flu-PSS was stronger than that of no-wrinkling surface without electrophoresis of Flu-PSS. (**Fig. 1-3**). This result suggests that PSS were deposited on cationic gel surface and formed polyion complex by electrophoresis. It is well known that wrinkle structures are formed by the generation of surface instability between two adhered layers[8-10]. These results suggest that the PIC layer was formed at the surface of hydrogels, and then wrinkle structures appeared because of the elasticity mismatch between hydrogel and PIC.

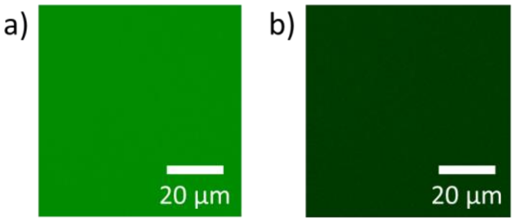

Fig. 1-3 Fluorescence microscopic observation of the hydrogel surface (a) with and (b) without electric field impression when Flu-PSS was used as anionic polymers.

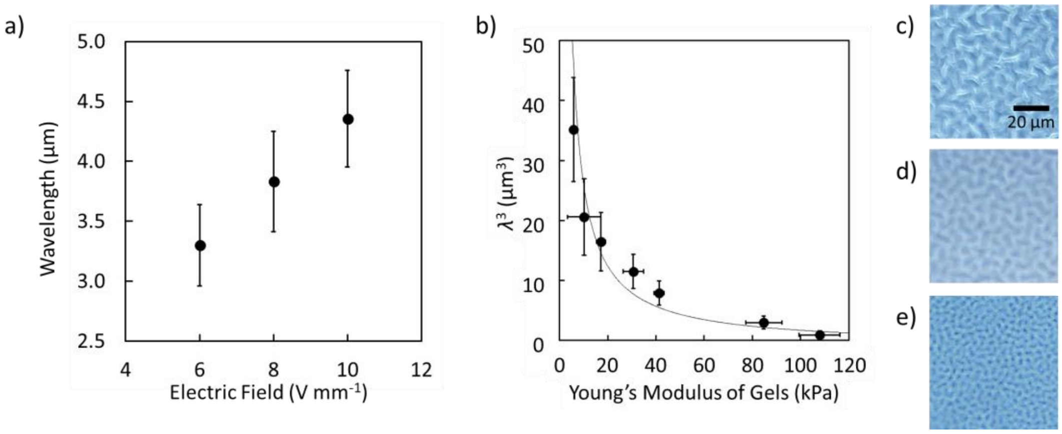

Fig. 1-4 (a) Wrinkle wavelength as a function of applied electric field during electrophoresis. Electrophoresis time was fixed at 5 sec. (b) Relationship between wrinkle wavelength and Young's modulus of gels. The black line trace the fitting curve. (c-e) Microscopic observation of wrinkled hydrogels. Their Young's moduli are (c) 5.8 kPa, (d) 30.6 kPa, and (e) 41.3 kPa, respectively.

The effect of electrophoresis condition was also evaluated because the PIC layer was formed by electrophoresis for ionic polymers. When the applied electric field during electrophoresis was changed, the wavelength of wrinkles was also changed (**Fig. 1-4a**). The wrinkle wavelength was increased with increasing the applied electric field. When the electrophoresis time was fixed at 5 s, wrinkles were not formed in the cases of the applied electric field was lower than 6 V mm^{-1}. The result indicates that wrinkle wavelength can be controlled by tuning the PSS concertation on the gel surface. As the concentration of PSS on cationic hydrogel increased, the thickness and/or the modulus of the PIC layer were considered to increase. The tendency of wrinkle wavelength to increase due to an increase in the thickness and/or modulus of PIC layer is also consistent with an equation that described the relationship between the wavelength of wrinkles and moduli of adhered layers (**eq. 1**).[11]

Moreover, wrinkle wavelength (λ) could be controlled by the Young's modulus of gels (E_S). Therefore, hydrogels with different cross-linking ratio were prepared to change their Young's moduli. The Young's moduli of gel were changed from 5.8±1.1 kPa to 107.9±8.5 kPa when the cross-linking ratio was changed from 0.3% to 2.0%. In fact, the wrinkle wavelength was strongly affected by E_s (**Fig. 1-4b-e**), resulting in the decrease in the wrinkle wavelength from 3.3 μm to 1.0 μm. This result agrees the tendency between wrinkle wavelength and Young's modulus of elastic substrate. As shown in **Fig. 1-4b**, the wrinkle wavelength is well fitted to an inverse function of E_s (**eq. 2**).

$$\lambda^3 = A/E_\mathrm{s} + B \qquad \textbf{(eq. 2)}$$

where A is $(2\pi t)^3 E_\mathrm{f} / 3 = 195$ and B is a fitting parameter equal to 2.2. From A and E_f, which is modulus of PIC layer, the PIC thickness t can be calculated. In this study, direct measurement of E_f and t is difficult. In another study, a PIC made with PDDA and PSS by layer-by-layer method, was reported and the Young's modulus is 590±90 MPa.[12] Therefore, t was calculated and with this modulus and the thickness was determined to be a few nanometers. Therefore, the origin of wrinkle structure formation was determined to be stress mismatch between the PIC constructed by electrophoresis and hydrogels.

This suggested that the wrinkle structure was fabricated by the formation of PIC layer at hydrogel surface. Since the PIC layer was formed by the application of electric field, it was possible to identify the pattern of the wrinkle structures by applying a selective electric field. As shown in **Fig. 1-5**, in the case of using electrodes patented on a curvature (**Fig. 1-5a**), a wrinkle structure transferred pattern was formed only the area that electric field was applied (**Fig. 1-5b**). There was no wrinkles formed at insulated part; thus, it was obvious that the wrinkle structure clearly patterned on the hydrogel surface

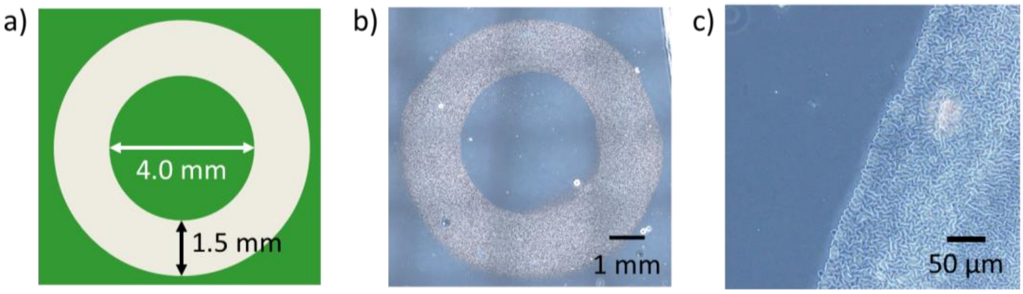

Fig. 1-5 (a) Illustration of insulating mask pattern of Pt electrodes. (b and c) Microscopic phase-contrast observations of (b) whole and (c) magnified of the boundary between wrinkle and flat surface.

(**Fig. 1-5c**). Moreover, this is a novel method for the wrinkle patterning at the surface of hydrogels compared to the photoresist method, which involves film formation with drying and light irradiation with photomasks, because the entire process can be performed in an aqueous environment without drying.

The wrinkle wavelength depended on the electrophoresis conditions because of the thickness and/or Young's modulus of PIC layer could be controlled by tuning the PSS concentration at hydrogel surface. Thus, electrodes was placed as sloped as shown in **Fig. 1-6a** and electrophoresis was carried out for fabrication of gradient wrinkle structures. In this case, both wavelength and amplitude of wrinkles gradually decreased from the left side to the right side, as shown in **Fig. 1-6b-d**. When electrodes were inclined, applied electric field intensity gradually decreased from left side to the right because the electric field depended on the distance between the cathode and the anode. Therefore, the author

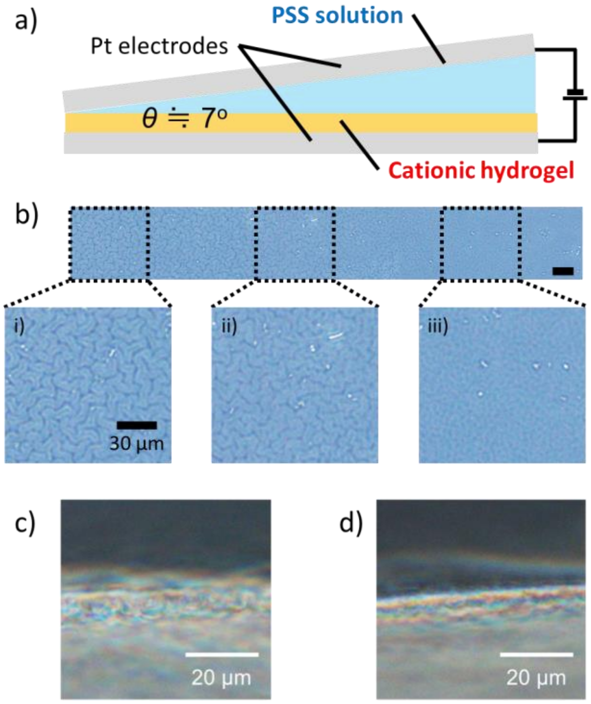

Fig. 1-6 (a) Experimental procedure of wrinkle structure formation with sloped electrodes. (b) Phase-contrast images of gradient wrinkle prepared by electrophoresis with sloped electrodes. (c and d) Cross-sectional images of gradient wrinkling surface. Observed areas were (c) (i) and (d) (iii), respectively.

considered that the wavelength of wrinkle structures continuously changed because the thickness and/or Young's modulus of PIC layer gradually changed. As a result, a gradient wrinkled hydrogel surface, which showed a continuous wavelength change, was fabricated utilizing sloped electrodes.

Usually, aligned wrinkles were formed by hard thin layer fabrication on the top of uniaxially or planarly stretched elastomers. Thus, electrophoretic wrinkle fabrication was performed to uniaxially stretched hydrogels (**Fig. 1-7a**). After electrophoresis, three types (random, herringbone and straight) wrinkle structures based on stretching ratio and/or Young's modulus of hydrogels, were observed at the surface of stretched hydrogels (**Fig. 1-7b-d**). A phase-diagram of wrinkle geometrical configurations is summarized in **Fig. 1-7e**. Regardless the Young's modulus, the wrinkle structures, which were random in cases of low or no stretching, tented to change into a herringbone and then to straight structure as the stretching ratio of hydrogels was increased. As shown in **Fig. 1-7c and d**, herringbone and straight wrinkles were aligned along the stretching direction of hydrogels. This result indicate that hydrogel surface was mainly buckled perpendicular to the stretching direction after PIC formation. These phenomena can be explained by the difference in the internal stress of the uniaxially stretched hydrogels between the stretching direction and perpendicular direction. Hydrogels tend to shrink perpendicular to the stretching direction in accordance with Poisson's ratio. It was reported that the internal stress of a gel under uniaxial or planar stretched was higher in the tensile direction than that of perpendicular direction.[13, 14] Since these aligned wrinkles were formed by stress mismatch between hydrogels and PIC layer, the wrinkles tend to become increasingly difficult to form as the gels were stretched. Therefore, herringbone

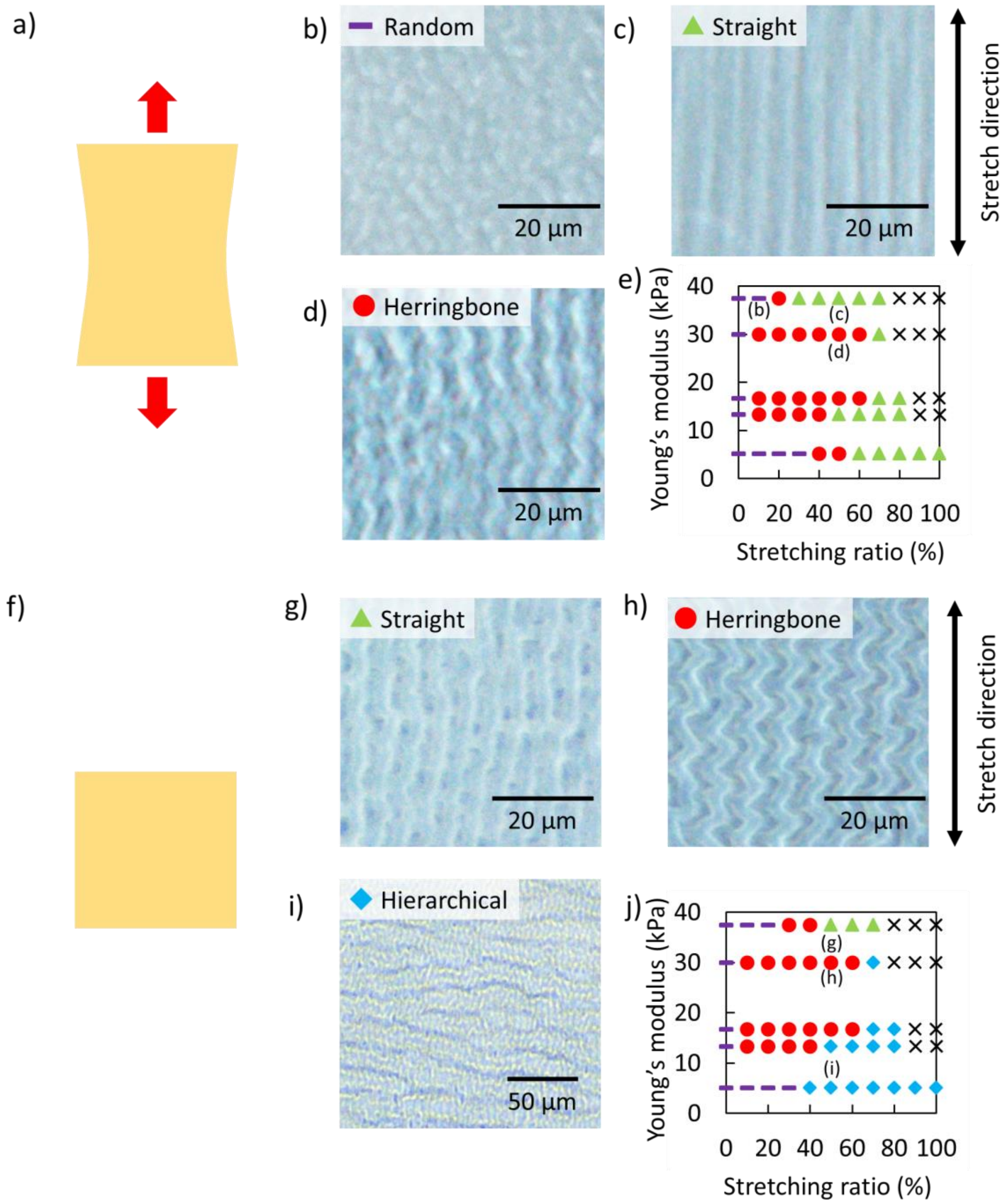

Fig. 1-7 (a) Schematic illustration of the top view of uniaxially stretched hydrogel. (b-d) Microscopic observations of wrinkle structures with (b) random, (c) straight, and (d) herringbone structures. (e) Phase-diagram of wrinkle structure formed after electrophoresis with stretching. Purple bar, green triangle, and red circle indicate random, straight, and herringbone wrinkle structures were formed after electrophoresis, respectively. Black cross indicates hydrogel was broken by stretching. (f) Schematic illustration of the top view of unloaded hydrogel. (g-i) Phase-contrast microscopic observations of hydrogels with (g) straight, (h) herringbone, and (i) hierarchical structures. (j) Phase-diagram of wrinkle structures after unloading. Purple bar, green triangle, red circle, and blue diamond indicate straight, aligned, herringbone, and hierarchical wrinkle structures were formed after unloading, respectively.

structure was formed when the stretching ratio is low, whereas straight form was observed for highly stretching. Chen and Hatchinson calculated the elastic energy of straight, herringbone and checkerboard shapes of wrinkle structures.[15,16] In these reports, the surface energy of her-ringbone wrinkle structure is the lowest because the her-ringbone shape is the only one among the three shapes that relaxes the in-plane stress in all directions without incurring significant stretch energy. Therefore, herringbone structures were formed with medium stretching. However, in cases of higher stretching, straight wrinkle structures were formed because the 3-D network of hydrogels were largely deformed, which meant that the relaxation of stress in the stretching direction was difficult. Moreover, the fact that a gel having a higher Young's modulus forms a straight structure with a lower stretching ratio also supports the present discussion. Some of these wrinkle structures changed their structure when unloaded (**Fig. 1-7f**). At the unloaded surfaces, four types (random, straight, herringbone and hierarchical) of wrinkle structures were observed (**Fig. 1-7g-i**). A phase-diagram of wrinkle geometrical configuration after unloading is shown in **Fig. 1-7j**. It is of especial interest that the aligned wrinkle which had a straight structure when stretched formed a new aligned wrinkle structure perpendicular to the stretching direction after unloading, resulting in a hierarchical wrinkle structure. The formation mechanism of the newly formed wrinkle perpendicular to the stretching direction is the same as the conventional method to form aligned wrinkles by unloading after formation thin hard film on stretched elastomer. In this study, it is possible to form aligned wrinkles under uniaxial stretching, and it is considered that a hierarchical wrinkle structure was formed by unloading.

Next, it was investigated that details of the herringbone structures, whose type of geometrical configuration do not change during stretching and after unloading. Typical microscopic observations of herringbone wrinkle structures during stretching and after unloading are shown in **Fig. 1-8a and b**. To investigate the effect of strain to the herringbone shape, the 1st and 2nd generation wrinkle wavelength (λ_{He} and Λ_{He}), the 2nd generation wrinkle angle (θ), and the 2nd generation wrinkle amplitude (A_{He}) were measured by phase-contrast microscopy. **Figure 1-8c and d** show λ_{He} and Λ_{He} as a function of stretching ratio of hydrogels, respectively. During stretching and unloading,

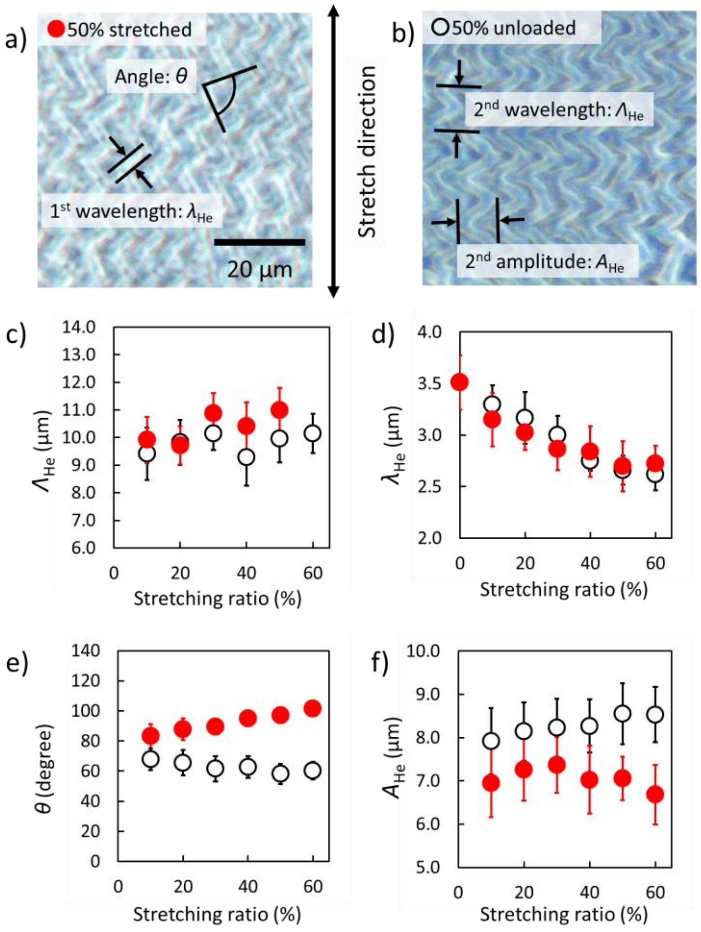

Fig. 1-8 (a, b) Microscopic observations of herringbone wrinkle structures on the surface of (a) stretched and (b) unloaded hydrogel. The modulus of hydrogel was 16.7±1.2 kPa. (c) 2nd generation wrinkle wavelength (Λ_{He}), (d) 1st generation wrinkle wavelength (λ_{He}), (e) 2nd generation wrinkle angle (θ) and (f) amplitude (A_{He}) as a function of stretching during electrophoresis.

neither λ_{He} nor Λ_{He} changed. The deformed 3-D network of hydrogels recovered its original shape after unloading. As expected, the herringbone angle θ decreased and Λ_{He} increased by unloading the stretched gels (**Figure 1-8e and f**).

The effect of stretching for hierarchical wrinkles was also investigated (Fig. 1-9). The 1st generation wrinkle wavelength (λ_{Hi}) and 2nd generation wrinkle wavelength (Λ_{Hi}) were measured as shown in **Fig. 1-9a and b**. As a result, neither λ_{Hi} nor Λ_{Hi} changed after the stretching ratio was changed (**Fig. 1-9c and d**). Here, the general relationship between wrinkle wavelength and Young's modulus of substrate was written above as **eq. 1**. From **Eq. 1**, wrinkle wavelength λ is predicted from t, E_f and E_s. The wavelength of the wrinkle structure decreases and converges as the Young's modulus increases. Therefore,

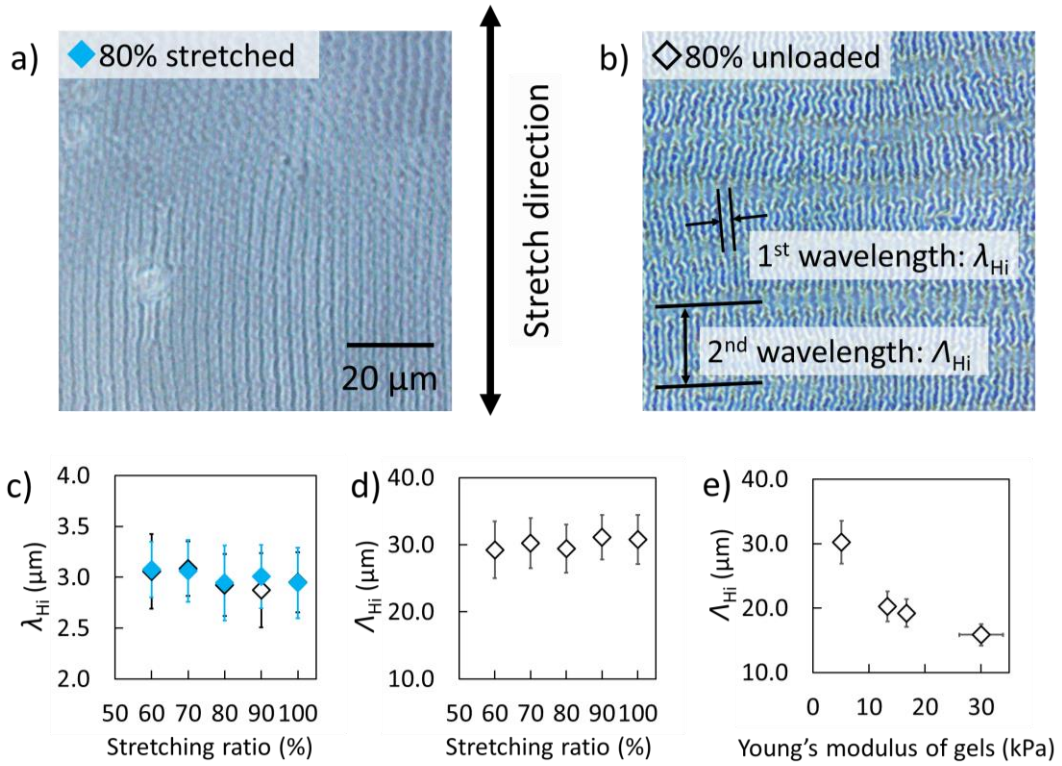

Fig. 1-9 (a, b) Microscopic observations of wrinkle structures at the surface of (a) stretched and (b) unloaded hydrogels. The modulus of hydrogel was 5.1±1.2 kPa. (c) 1st generation wrinkle wavelength (λ_{Hi}) and (d) 2nd generation wrinkle wavelength (Λ_{Hi}) of hierarchical wrinkles as a function of stretch. (e) 2nd generation wrinkle wavelength (Λ_{Hi}) hierarchical wrinkles as a function of Young's modulus of gels. Stretching ratio for each gels was 70%.

it seems that the λ_{Hi} did not change because hydrogel was sufficiently stretched. Also, A_{Hi} was not changed by changing the stretching ratio. However, by changing the Young's modulus of hydrogels, A_{Hi} decreased with increasing Young's modulus (**Fig. 1-9e**). This result agrees with the relationship written in **Eq. 1**. Therefore, 2nd generation wrinkle structure was formed by stress mismatch between the hard PIC layer and the soft hydrogel caused by stretch release.

Finally, geometry control of wrinkle structures on the stimuli-responsive hydrogels was tried. PNIPAAm hydrogel, is known as a thermo-responsive hydrogel.[17] PNIPAAm gel swelled in water at temperatures below 32 °C, so-called the lower critical solution temperature (LCST), however it shrunk with water release at temperatures above the LCST. The Young's modulus of the PNIPAAm gel increased above LCST due to the aggregation of polymer chains (**Fig. 1-10**). It was found that the shapes of wrinkle structure on the gel surface varied depending on the elastic modulus of the gel as shown in **Fig.1-11**. Therefore, it was possible to create a stimuli-responsive, shape transformable wrinkled surface by controlling the elastic modulus of the PNIPAAm gel in response to an external stimulus (**Fig. 1-11a, left**). Interestingly, the observed wrinkle structure disappeared by increasing the temperature to 50 °C (**Fig. 1-11a, right**). This process is

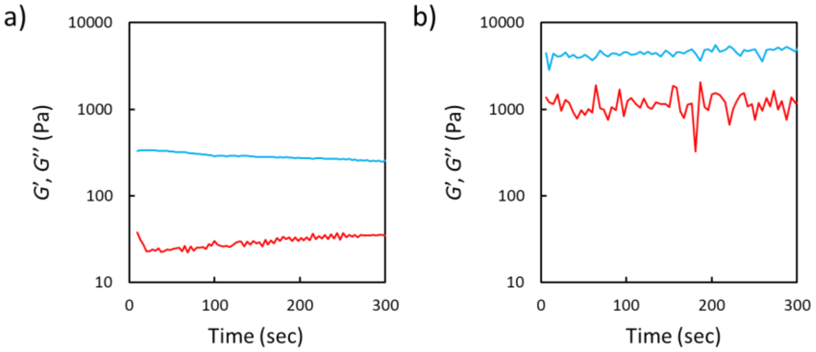

Fig. 1-10 (a, b) Temporal evaluation of storage modulus (*G*', blue lines) and loss modulus (*G*'', red lines) of PNIPAAm gel followed using rheology. The measuring temperature was (a) 20 °C and (b) 40 °C, respectively. The frequency and the thickness of hydrogel were 1 Hz and 0.6 mm, respectively.

found to be reversible, because wrinkle structure reappeared by decreasing the temperature below LCST. As described above, the wrinkle structure was generated by the stress mismatch between gels and PIC layer at lower temperature. However, Young's modulus of PNIPAAm gel increases above to LCST due to aggregation of polymer chains. It is confirmed that Young's modulus of PNIPAAm gel increased above LCST (**Fig. 1-10**). During this process, the size of PNIPAAm gel is hardly changed (inset image of **Fig. 1-11a**). Thus, the wrinkle deformation did not caused by dehydration of PNIPAAm hydrogels triggered by temperature increasing. In addition, as shown in **Fig, 1-11b**, the author confirmed that the herringbone wrinkle structures formed on the PNIPAAm gel below LCST (**Fig. 1-11b, left**) transformed to straight shape when the temperature was increased to 50 °C (**Fig. 1-11b, right**). This process was found to be reversible, the herringbone structure reappeared when the temperature was decreased below LCST. As described above, the kind of wrinkle geometrical configuration was changed by the Young's modulus of hydrogels. After increasing the temperature of hydrogels above LCST, the modulus of hydrogels increased due to polymer aggregation. Therefore, geometrical configuration of the wrinkles was changed by temperature increasing above LCST. Similarly, the hierarchical wrinkle also reversibly changed their geometry in response to temperature (**Fig. 1-11c**). It was succeeded in developing a stimuli-responsive hydrogel wrinkle that changes geometry by external stimulation.

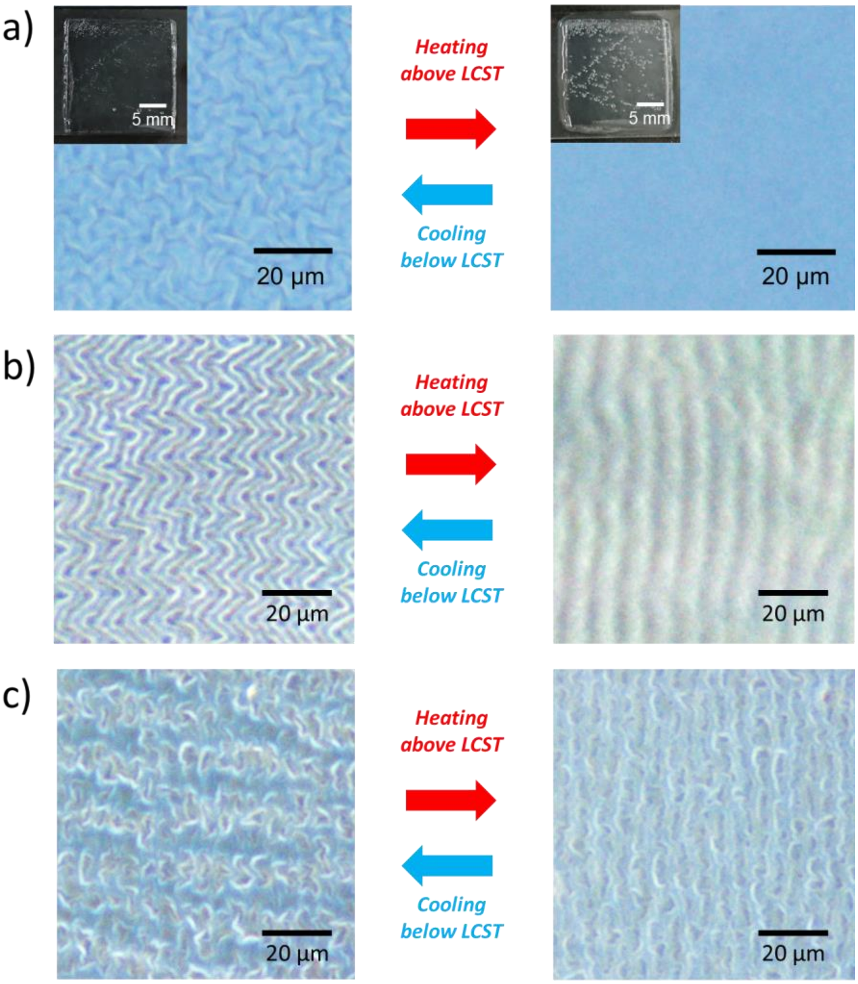

Fig. 1-11 (a) Phase-contrast microscopic observations of stimuli-responsive wrinkle structures at the surface of PNIPAAm hydrogel. The temperature of hydrogel was (left) 20 and (right) 50 °C, respectively. Inset images are PNIPAAm gels. (c) Thermoresponsive transformation of (a) herringbone and (b) hierarchical wrinkle structures. The temperature was jumped between (left) 20 °C and (right) 50 °C.

1.4 Conclusion

In conclusion, a novel method for fabrication of wrinkled hydrogel surface in aqueous condition was developed using electrophoresis. Wrinkle surface was fabricated by formation of PIC layer on hydrogels using electrophoresis. Wrinkling wavelength was able to control by changing an electrophoresis condition and Young's modulus of hydrogels. By using patterned and sloped electrode, the patterned and gradient wrinkle surface on the hydrogels were prepared. Moreover, aligned wrinkle structures were fabricated at the surface of stretched hydrogels by the electrophoretic wrinkle fabrication method. After electrophoresis, three types of wrinkle geometry (random, straight and herringbone) were observed on the surfaces of stretched hydrogels. The geometrical configuration was changed by changing the modulus of the hydrogels and/or stretching ratio during electrophoresis. After unloading the stretching, a hierarchical wrinkle structure was fabricated. The effect of stretching ratio and Young's modulus of hydrogels for aligned wrinkle structures was investigated through their wavelength, amplitude and herringbone angles. Active wrinkles which can switch their shape by external stimulus, was also fabricated by the formation of PIC layer on surface of thermoresponsive hydrogel. Stimuli-responsive wrinkle surface could be switched their wrinkle shapes by changing the modulus of hydrogels triggered by varying temperature. Because this wrinkle formation method is very simple and PIC layer can be formed easily at the surface of hydrogel, the present wrinkle hydrogel surface will be useful as a novel platform for selective manipulation of micro-scale soft objects.

1.5 References

1. Y. Tokudome, K. Suzuki, T. Kitanaga, M. Takahashi. *Sci. Rep.* **2012**, *2*, 683.
2. Z. Zhao, j. Gu, Y. Zhao, Y. Guan, X. X. Zhu, Y. Zhang. *Biomacromolecules* **2014**, *15*, 3306-3312.
3. M. Ebara, K. Uto, N. Idota, J. M. Hoffman, T. Aoyagi. *Adv. Mater.* **2012**, *24*, 273–278.
4. K. Matsukawa, T. Masuda, Y. S. Kim, A. M. Akimoto, R. Yoshida. *Langmuir* **2017**, *33*, 13828-13833.
5. Y. Tokudome, H. Kuniwaki, K. Suzuki, D. Carboni, G. Poologasundarampillai, M. Takahashi, *Adv. Mater. Interfaces* **2016**, *3*, 1500802
6. Y. Takemoto, H. Ajiro, T. Asoh, M. Akashi. *Chem. Mater.* **2010**, *22*, 2923-2929.
7. J. J. Richardson, M. Björnmalm, F. Caruso. *Science* **2015**, *348*, 411.
8. N. Gao, X. Xhang, S. Liao, H. Jia, Y. Wang. *ACS Macro Lett.* **2016**, *5*, 823-827.
9. E. P. Chan, E. J. Smith, R. C. Hayward, A. J. Crosby. *Adv. Mater.* **2008**, *20*, 711-716.
10. A. E. Schedl, C. Neuber, A. Fery, H. Schmidt. *Langmuir* **2018**, *34*, 14249-14253.
11. S. Yang, K. Khare, P. C. Lin, *Adv. Funct. Mater.* **2010**, *20*, 2550-2564.
12. B. Wu, C. Li, H. Yang, G. Liu, G. Zhang. *J. Phys. Chem. B* **2012**, *116*, 3106-3114.
13. Y. Bitoh, K. Urayama, T. Takigawa, K. Ito. *Soft Matter* **2011**, *7*, 2632-2638.
14. M. Fujine, T. Takigawa, K. Urayama. *Macromolecules* **2015**, *48*, 3622-3628.
15. T. Mai, Y. Morishita, K. Urayama. *Polymer* **2017**, *126*, 29-39.
16. X. Chen, J. W. Hatchinson. *J. Appl. Mech.* **2004**, *771*, 597-603.
17. X. Chen, J. W. Hatchinson. *Scr. Mater.* **2004**, *50*, 797-801.
18. Y. Hirokawa, T. Tanaka. *J. Chem. Phys.* **1984**, *81*, 6379.

Chapter 2.

Hydrogel Adhesion with Wrinkle Formation by Spatial Control of Polymer Networks

2.1 Introduction

Wrinkle structures are often observed around soft and elastic interfaces such as brain, fingers in human body and play an important role in increasing the surface area. It is well-known that wrinkles are formed by the generation of surface instability of elastic materials,[1-5] indicating that a wrinkles have potential applications in the adhesion of two soft materials. In fact, the formation of such wrinkles which can adhere two materials were reported utilizing surface-treated elastomers[1,2] and has been used for dry-adhesive substrates[3] using the enhanced surface.

On the other hand, hydrogels are similar to macromolecular-based constituents such as proteins, cells and tissues. Therefore, hydrogel adhesion has numerous applications for next-generation material creation such as artificial tissues,[6] drug delivery systems,[7] and elastic actuators.[8] Thus, hydrogel adhesion method are required, and researched using interactions such as electrostatic,[9-11] host-guest,[12] metal-ligand,[13,14] and organic-inorganic[15-17] interactions. In these methods, interactive units around the outmost surface of hydrogels play an important role in hydrogel adhesion. However, the stoichiometric investigation of interactive units for the adhesion is the central part of discussions. The spatial arrangement of interactive units based on the polymer network design was mostly unknown. Moreover, wrinkle structures were formed at the surface of hydrogels using surface-swelling[18-19] or drying.[20] There are no guideline for the chemical design and interactive units.

In this chapter, it was focused on the spatial control of polymer networks such as density, distribution, and mobility of interactive units for a wrinkle structure at adhered hydrogel interface. The role of wrinkle structures at adhesive interface of hydrogels was investigated by the measurement of adhesive strength of hydrogels which are adhered under compression.

2.2 Experimental Section

Materials.

N,N-Dimethylacrylamide (DMAAm) was purchased from FUJIFILM Wako Pure Chemical Corporation and used after distillation. 2,2'-Azobis[2-(2-imidazolin-2-yl)-propane]dihydrochloride (VA-044), ammonium persulfate (APS), *N*,*N*'-methylenebis (acrylamide) (MBAAm), *N*,*N*,*N*',*N*'-tetramethylethlenediamine (TEMED), and [3-(methacryloylamino)propyl]trimethylammonium chloride (TMA) were purchased from FUJIFILM Wako Pure Chemical Corporation and used as purchased without further purification. Sodium styrenesulfonate (SSNa) and sodium poly(styrenesulfonate) (PSS) were purchased from Aldrich and used as purchased without further purification. Poly(diallyldimethylammonium chloride) (PDDA) was purchased from Aldrich and used after freeze drying.

Preparation of hydrogels.

The copolymerization of SSNa and DMAAm with MBAAm was carried out in water using 1 mol % APS as an anionic radical polymerization initiator and TEMED at 4 °C for 8 h. For the preparation of cationic TMA copolymer gels, VA-044 was used as a cationic azo-initiator and then gelation was carried out at 40 °C for 8 h. Semi-interpenetrating polymer networks (semi-IPNs) were prepared by the free-radical polymerization of DMAAm with MBAAm in the presence of PSS or PDDA by using an anionic or cationic initiator. The prepared hydrogel was washed with water for the removal of unreacted monomer. Young's modulus was measured using a tensile tester (EZ-S10, Shimadzu) in an ambient atmosphere. They were loaded to failure at 3 mm min^{-1} in tensile mode.

Hydrogel adhesion.

The hydrogel adhesion was carried out using electrophoretic hydrogel adhesion method.[21-23] Briefly, electrophoresis was carried out between two Pt electrodes. The two gels were held in contact with each other between the Pt electrodes, and an electric field was applied. In this case, cationic gels were on the anode and anionic gels were on the cathode. The applied voltage and electrophoresis time were 5 V mm^{-1} and 3 s, respectively. The lap shear adhesion force was measured using a tensile tester in an ambient atmosphere. The adhered gels were loaded to failure at 3 mm min^{-1} in tensile mode, and the failure strain was measured. The adhered interfaces were observed by phase-contrast microscopy (IX-73, Olympus).

2.3 Results and Discussion

Two types of hydrogels (a copolymer gel and semi-interpenetrating polymer networks (semi-IPNs)), which have structures charged groups were chemically and physically fixed on the network, were prepared (**Fig. 2-1**). The charge density of hydrogels was controlled by the amount of charged monomer and polymers. The adhesion of hydrogels was carried out by previously reported electrophoretic adhesion method (**Fig. 2-2**). During electrophoresis, cationic and anionic polymer chains move to the cathode and anode, respectively, and polyion complexes (PIC) were eventually formed at the hydrogel interface, causing adhesion. As shown in **Fig. 2-3a**, two hydrogels quickly adhered within 3 s, and adhesive interfaces were visually transparent. Interestingly, wrinkle structure was founded at only adhered semi-IPNs hydrogel interfaces by phase-contrast microscopic observation (**Fig. 2-3b**).

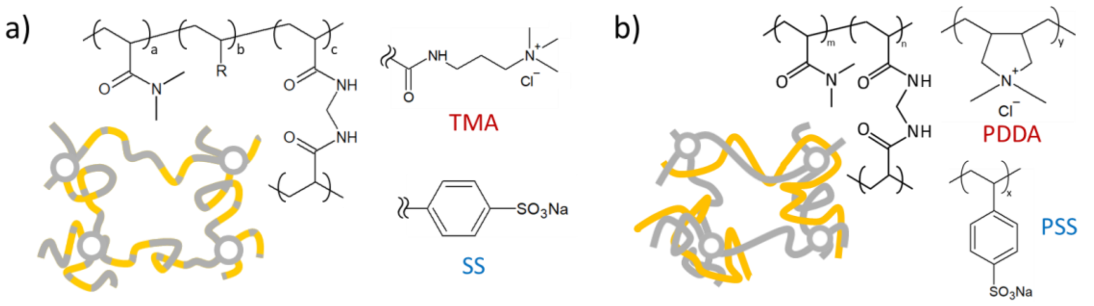

Fig. 2-1 Schematic illustrations and chemical structures of (a) copolymer and (b) semi-IPNs hydrogels and their ionic groups.

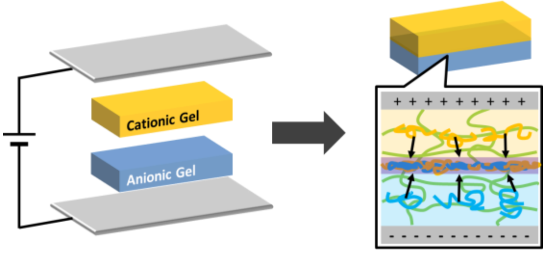

Fig. 2-2 Schematic illustration of electrophoretic adhesion method for hydrogels.

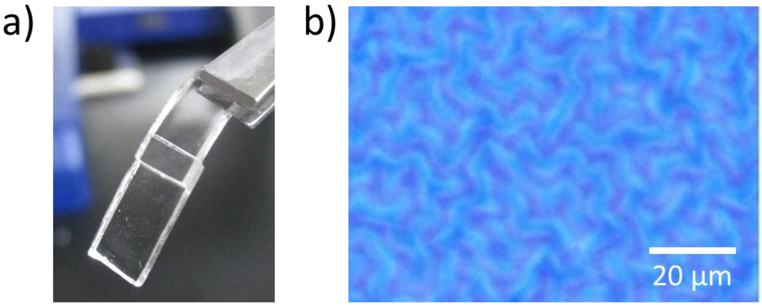

Fig. 2-3 (a) Macroscopic and (b) microscopic observations of adhered semi-IPNs by electrophoretic method.

To investigate the relationship between the wrinkle structure and adhesive strength, the lap shear adhesion force was measured (**Fig. 2-4a**). The adhesive strength of semi-IPNs and copolymers gels is shown in **Fig. 2-4b**. The adhesive strength of both gels increased with increasing ionic monomer units inside polymer networks. The adhesive strength of semi-IPNs was stronger than that of copolymer gels in all cases. These results indicate that the adhesion of hydrogels was controlled by the amount of charged monomer and also depended on the network structure, especially on the local charge density of gel networks. The charge densities of both copolymer gels and semi-IPNs were normalized

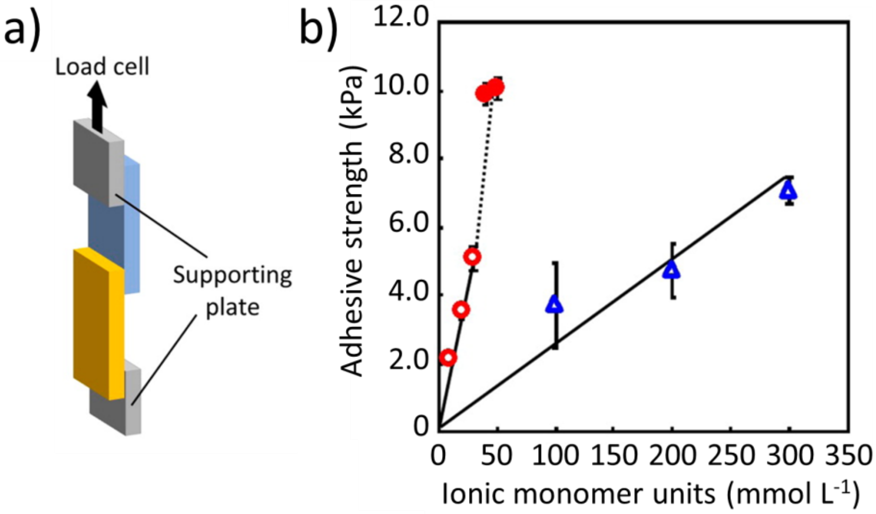

Fig. 2-4 (a) Experimental procedure of lap-shear adhesion test on adhered cationic and anionic hydrogels. (b) Adhesive strength of semi-IPNs hydrogels (red circle) and copolymer hydrogels (blue triangle) as a function of introduced ionic momomer units concentration. Closed symbols indicate gels were broken during tensile test before detachment .

by the molarity of ionic monomer units. When the copolymer gels and semi-IPNs have the same extent of charge density, charged units inside the copolymer gels may be uniformly dispersed inside the PDMAAm networks. However, semi-IPNs have higher and lower local charge densities because of the presence of linear PSS or PDDA inside the networks. When the ionic monomer units have concentrations of 40 and 50 mmol L^{-1} for semi-IPNs, the adhesion interface with wrinkles was stronger than the gels themselves, and the gels were broken before the adhesion interface detached during a tensile strength test (**Fig. 2-4b**, closed circle; **Fig. 2-3b**). Stronger adhesion seems to be due to the formation of PIC films as an adhesive layer during electrophoresis. Therefore, wrinkle formation was observed for semi-IPNs with 30 mmol L^{-1} ionic monomer units, although a wrinkle was not formed for copolymers gel with 300 mmol L^{-1} ionic monomer units and semi-IPNs with 10 mmol L^{-1} ionic monomer units. These results indicate that a buckling instability did not occur because of an insufficient PIC layer due to lower polymer mobility and poor charge density. Moreover, similar behavior in adhesive strength was observed even though the concentration of ionic monomer units of copolymer gels is 10-fold higher than for semi-IPNs, indicating that the amount of charge, charge density, mobility of polymer networks, and wrinkle formation are important for the strong adhesion of hydrogels. In addition, wrinkle structures were not formed without electrophoresis in all cases. Therefore, wrinkles at adhered interface were fabricated by electrophoresis.

Generally, interface wrinkles are formed by stress mismatch between adhered two layers and their relationship is written as **eq. 1** as below. Thus, in this case, the cross-linking ratio of hydrogels was changed to modulate E_s. When the cross-linking ratio was changed from 1.0% to 0.3%, the Young's moduli of gels were changed from 520±90 kPa to 115±30 kPa. Actually, the size of wrinkle structures were strongly affected by E_s (**Fig. 2-5**). As shown in **Fig. 2-5e**, the wrinkle wavelength was well fitted with an inverse function of E_s (**Eq. 2**) and $A = 1.3 \times 10^4$ and $B = 28$. Direct measurement of PIC layer at adhered hydrogel interface is difficult but the author calculated with the reported PIC modulus as chapter 1. The PIC thickness was calculated a few hundred nanometers. Cross-sections of adhered hydrogels were also confirmed because phase contrast images may just reveal a periodic variation in the refractive index of PIC layers and hydrogels. The no-wrinkle interface showed a flat cross-section (**Fig. 2-6a**). However, a waving adhesive interface was observed at a cross-section of wrinkle interfaces and amplitude showing an increasing tendency with decreasing cross-linking ratio of hydrogels (**Fig. 2-6b, c**). These results strongly suggested that wrinkles at interfaces had three-dimensional structure.

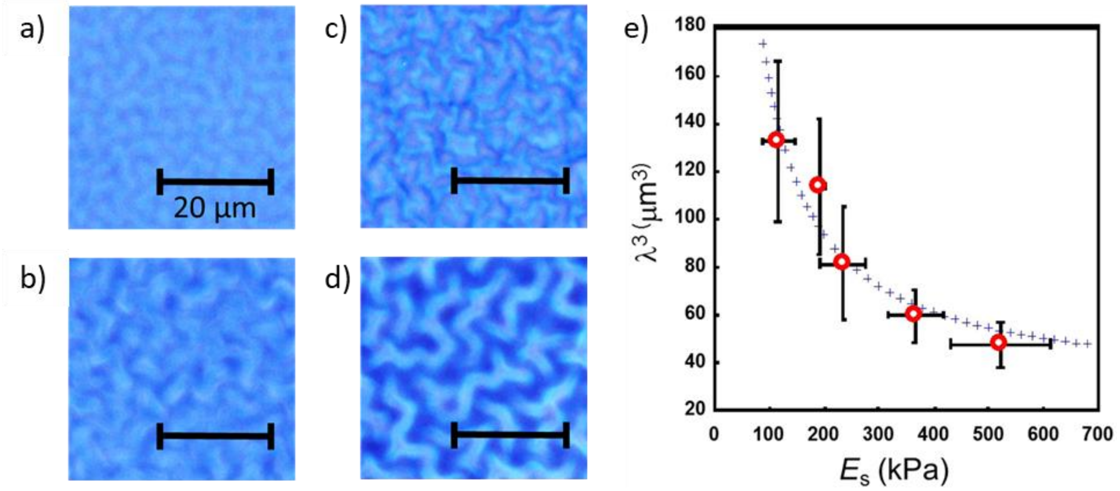

Fig. 2-5 (a-d) Phase-contrast microscopic images of adhered 50 mmol L^{-1} semi-IPNs. The cross-linking ratio of each gels were (a) 1.0%, (b) 0.7%, (c) 0.5%, and (d) 0.3%, respectively. (e) Relationship between wrinkle wavelength (λ) and Young's modulus of gels (E_s). Plus symbols trace the fitting curve.

Finally, to investigate the role of wrinkle structure in adhesion, the adhesive strength of hydrogels when electrophoretic adhesion was carried out under the compression of hydrogels, was measured because a wrinkle was formed by vertical

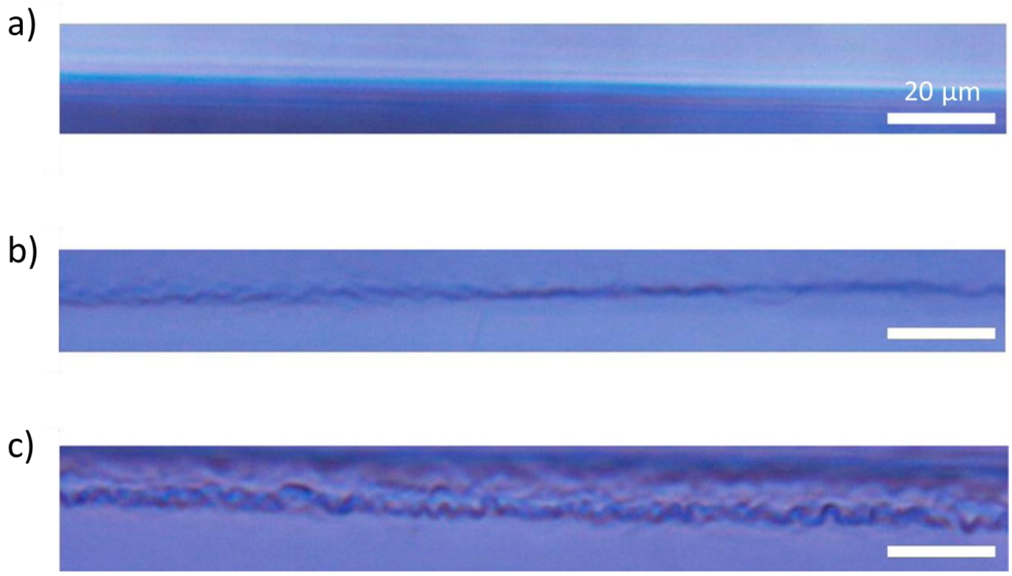

Fig. 2-6 Cross-section images of adhered (a) 10 mmol L^{-1} and (b, c) 50 mmol L^{-1} semi-IPNs. Cross-linking ratio values of (a, b) and (c) are 1.0% and 0.3%, respectively.

growth with horizontal shrinking. It was hypothesized that wrinkle formation was inhibited by the deformation of hydrogels as a result of vertical compression and horizontal stretching. Therefore, electrophoretic adhesion was carried out under compression, and adhesive strength was measured after stress release. The compression ratio was calculated from the height of two gels without (h_0) and with (h) compression (**Fig. 2-7a**). 20, 30, 40, and 50 mmol L^{-1} semi-IPNs were used for the measurement. In the cases of 20 and 30 mmol L^{-1}, a significant difference was not observed for adhesive strength with and without compression (**Fig. 2-7b**, squares and inverse triangles). In the case of 50 mmol L^{-1} semi-IPNs, wrinkle structures were clearly observed from 0 to 23% compression, and then the gels were broken before the adhesion interface detached. When the hydrogels were compressed to 42%, the detachment of adhered gels and the disappearance of wrinkle structure was observed (**Fig. 2-7b**, circles). The fracture of both the adhesive interface and gel itself occurred between 23 and 42% compression. These results indicate that wrinkle formation is inhibited by hydrogel compression. Generally, two materials adhered by compression as a result of close contact with each other. On the contrary, in the present system, it was found that the deformation of hydrogel networks inhibited wrinkle formation, and then the adhesive strength decreased. Therefore, increasing the compression ratio resulted in a decrease in the adhesive strength of 40 mmol L^{-1} semi-IPNs in a continuous manner (**Fig. 2-7b**, triangles) with the disappearance of wrinkle structure (**Fig. 2-7c and d**). These results indicate that strong hydrogel adhesion was achieved by both the chemical design of interactive units and interface relaxation such as wrinkle formation.

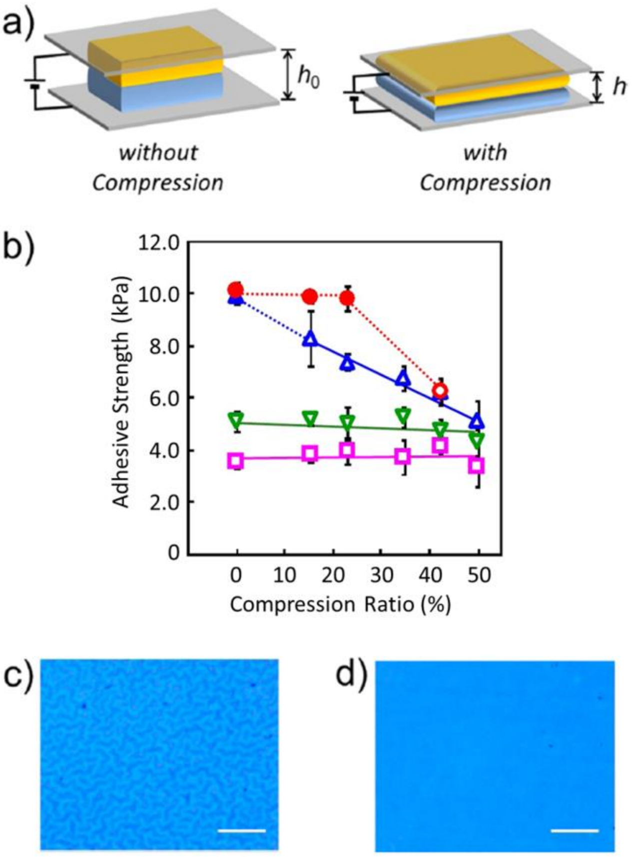

Fig. 2-7 (a) Electrophoretic adhesion under the compression of gels and (b) adhesive strength of hydrogels as a function of the compression ratio. Circles, triangles, inverse triangles, and squares indicate 50, 40, 30, and 20 mmol L−1 semi-IPNs. The closed symbols show where the adhered gels have broken. (c, d) Phase-contrast microscopic observation of adhered 40 mmol L−1 semi-IPNs gels with (c) 0 and (d) 50% compression. All scale bars are 20 µm.

2.4 Conclusion

A novel adhesive interface for hydrogels with a wrinkle structure was fabricated *via* spatial control of polymer networks. The author confirmed that the wrinkle structure at adhesive hydrogel interfaces was formed by the elasticity mismatch of hydrogels and PIC layers. Wrinkling wavelengths were strongly affected by Young's modulus of hydrogels, resulting in the wrinkling wavelength increasing with a decreasing Young's modulus of hydrogels. Increasing the compression ratio of hydrogels resulted in a decrease in the adhesive strength with wrinkle disappearance. It was suggested that the presence of wrinkle structure strengthens the adhesive strength of hydrogels. The discovery of wrinkle structure at the adhesive interface will contribute considerably to the development of a novel adhesion strategy and an understanding of interfaces of soft materials.

2.5 References

1. H. S. Kim, A. J. Crosby. *Adv. Mater.* **2011**, *23*, 4188-4192.
2. Y. Tokudome, K. Suzuki, T. Kitanaga, M. Takahashi. *Sci. Rep.* **2012**, *2*, 683.
3. E. P. Chan, E. J. Smith, R. C. Hayward, A. J. Crosby. *Adv. Mater.* **2008**, *20*, 711-716.
4. M. Guvendiren, S. Yang, J. A. Burdick. *Adv. Funct. Mater.* **2009**, *19*, 3038-3045.
5. M. Guvendiren, J. A.Burdick, S. Yang. *Soft Matter* **2010**, *6*, 2044-2049.
6. K. Y. Lee, D. J. Mooney. *Chem. Rev.* **2001**, *101*, 1869-1879.
7. T. Vermonden, R. Censi, W. E. Hennink. *Chem. Rev.* **2012**, *112*, 2853-2888.
8. J. Shang, X. Le, J. Zhang, T. Chen, P. Theato. *Polym. Chem.* **2019**, *10*, 1036-1055.
9. H. Tamagawa, F. Nagato, S. Umemoto, M. Okui, S. Popovic, M. Taya. *Bull. Chem. Soc. Jpn.* **2002**, *75*, 383-388.
10. H. Tamagawa, Y. Takahashi. *Mater. Chem. Phys.* **2008**, *107*, 164-170.
11. H. Abe, Y. Hara, S. Maeda, S. Hashimoto. *Chem. Lett.* **2014**, *43*, 243-245.
12. A. Harada, R. Kobayashi, Y. Takashima, A. Hashidzume, H. Yamaguchi. *Nat. Chem.* **2011**, *3*, 34-37.
13. N. Holten-Andersen, M. J. Harrington, H. Birkedal, B. P. Lee, P. B. Messersmith, K. Y. C. Lee, J. H. Waite. *Proc. Natl. Acad. Sci. U. S. A.* **2011**, *108*, 2651-2655.
14. T. Asoh, H. Yoshitake, Y. Takano, A. Kikuchi. *Macromol. Chem. Phys.* **2013**, *214*, 2534-2539.
15. K. Haraguchi, K. Uyama, H. Tanimoto. *Macromol. Rapid Commun.* **2011**, *32*, 1253-1258.
16. Q. Wang, J. L. Mynar, M. Yoshida, E. Lee, M. Lee, K. Okuro, K. Kinbara, T. Aida. *Nature* **2010**, *463*, 339-343.

17. S. Rose, A. Prevoteau, P. Elziére, D. Hourdet, A. Marcellan, L. Leibler. *Nature* **2014**, *505*, 382-385.
18. J. Hou, Q. Li, X. Han, C. Lu. *J. Phys. Chem. B* **2014**, *118*, 14502-14509.
19. F. Weiss, S. Cai, Y. Hu, M. K. Kang, R. Huang, Z. Suo. *J. Appl. Phys.* **2014**, *114*, 073507.
20. H. Izawa, Y. Miyazaki, T. Yonemura, N. Ito, Y. Okamoto, S. Ifuku, M. Morimoto, H. Saimoto. *Polym. J.* **2019**, *51*, 675-683.
21. T. Asoh, A. Kikuchi. *Chem. Commun.* **2010**, *46*, 7793-7795.
22. T. Asoh, W. Kawai, A. Kikuchi. *Soft Matter* **2012**, *8*, 1923-1927.
23. T. Asoh, E. Kawamura, A. Kikuchi. *RSC Adv.* **2013**, *3*, 7947-7952.

Chapter 3.

Hydrogel Adhesion with Wrinkling Films

3.1 Introduction

Adhesion is an essential process to build 3-D architectures for all materials regardless of soft or hard materials, which have been achieved by chemical[1-3] and physical[4-6] approrches. Among of them, adhesion control for hydrogels is still challenging task because hydrogel is one of the most difficult materials to adhere each other due to their high water contnet. For hydrogel adhesion, focus was made on chamical approrches, that is, intermolecular interactions such as ionic bonding,[7,8] host-guest interaction[9] and metal-ligand interaction.[10,11]

In the chapter 2, wrinkle structure was formed at adhered gel-gel interface by PIC formation as adhesive layer, and it was founded that wrinkle structure at the interface of adhered hydrogel has a ability strengthening the adhesion.[12] Generally, wrinkle structures are generated by stress-mismatch around the surface and interior of elastic materials.[13-15] Therefore, the wrinkle structue at the adhered interface was formed by stress-mismatch between PIC as adhesive layer and hydrogels as substrates. The discovery of wrinkles at adhesive interface will contribute consicerbly to the development of a novel adhesion strategy and an understanding of the interfaces of soft materials.

Focusing on the fine structure of the interface, microstructured hydrogel surfaces were used for reversible adhesion to hard materials.[16] In this report, octopus-like adhesive pads which were prepared by using thermoresponsive hydrogels showed pressure-induced adhesion in response to temperature. Gong *et al*. reported hydrogels which show fast, strong, and reversible underwater adhesion by combination of macroscopic surface engineering and tough hydrogels with dynamic bonds.[17] Microstructures on gel surfaces would open new science and technology for soft interfaces; however, such physical approaches to hydrogel adhesion to each other had been rarely reported to the best of our knowledge.

In chapter 3, a novel adhesion control system for hydrogels is proposed utilizing stimuli-responsive wrinkle structures at the interface of adhered hydrogels. Wrinkle structures were simply formed by water uptake of dried-gel film at the adhered interface of hydrogels (**Fig 3-1**). The role of interface structures was investigated using three types of interface structures. An aligned wrinkle structure was formed using an anisotropic swellable film. In the stress–strain test for adhered hydrogels, the deformation of wrinkle structure caused by external force decreased the adhesion strength of hydrogels. Wrinkle structures at the strongly adhered interface were deformed by peeling off of the wrinkled film, and adhered gels were detached with no damage to their surfaces. A demonstration of the adhesion control for hydrogels was carried out using a thermoresponsive hydrogel film.

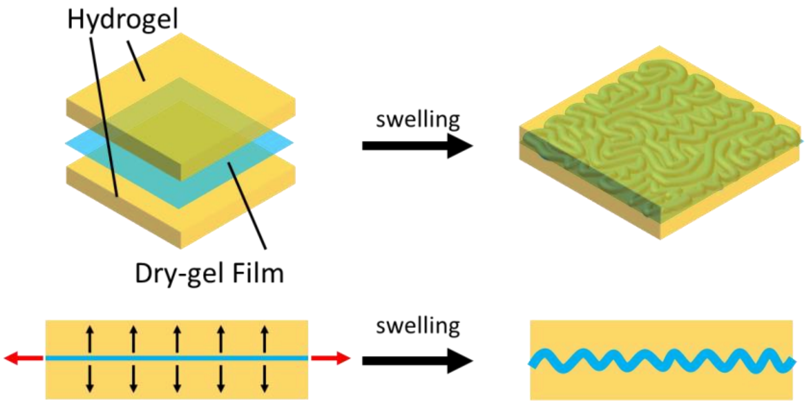

Fig. 3-1 Schematic illustration of hydrogel adhesion with wrinkled gel film.

3.2 Experimental Section

Materials.

Poly(vinyl alcohol) (PVA, polymerization degree = about 2000, saponification degree = 98.5%) was purchased from NACALAI TESQUE, Inc. and used as purchased. 1 mol L^{-1} hydrochrolic acid, 25% glutarldehyde solution and 90% acetaldehyde solution were purchased from FUJIFILM Wako Pure Chemical Corporation and used as purchased. Sodium poly(4-styrenesulfonate) (PSS) was purchased from Aldrich and used as purchased without further purification. Poly(diallyldimethylammonium chloride) (PDDA) was purchased from Aldrich as aqueous solution and used after freeze dried.

Preparation of PVA gels and films.

PVA (2.0 g) was dissolved into water (20 mL). Then, 25% glutaraldehyde solution (86 μL) and 1 mol L^{-1} hydrochloric acid (400 μL) were added for the preparation of PVA hydrogels (**Scheme 3-1**). To prepare cationic or anionic gel films, cross-linking reaction was performed under the presence of PDDA as cationic polymer or PSS as anionic polymer. Ionic monomer unit concentration was fixed to 30 mmol L^{-1}. Pre-gel solution was poured into a mold made with 10 x 10 cm^2 glass plates and 2 mm thickness silicon elastomer as a spacer; then they were placed in atmosphere for 24 h at room

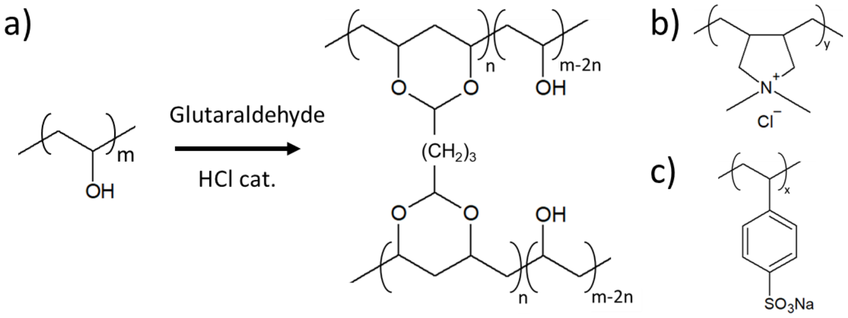

Scheme 3-1 (a) Preparation of PVA hydrogel by cross-linking reaction. (b and c) Chemical structure of (b) cationic PDDA and (c) anionic PSS.

temperature for cross-linking reaction. Anionic PVA gels were prepared as thin films using 50 μm thickness Teflon spacer. All prepared gels and films were immersed in pure water to remove unreacted chemicals and used after reaching equilibrium swelled state. Washed anionic hydrogel films were shrunken in ethanol–water mixture as poor solvent. To change the shrinking ratio, the mixture ratio of ethanol and water was changed. After shrinking process, they were vacuum dried on glass plate. Before use in adhesion experiments, cationic hydrogels and dried anionic hydrogel films were cut into 25 x 10 mm^2 and 2.5 x 10 mm^2, respectively.

Adhesion of cationic PVA gels with anionic PVA hydrogel films.

Adhesion of cationic PVA hydrogels was carried out by sandwiching of dried anionic film with two pieces of cationic hydrogels, and then they were immersed in water for 24 h. Adhered interfaces were observed by phase-contrast microscope (IX-73, Olympus). Lap-shear adhesion test for adhered hydrogels was performed using tensile tester (EZ Graph, Shimadzu) and adhesion strength was measured as shear stress. The tensile speed was 120 mm min^{-1} in atmosphere.

Preparation of LCST-type thermoresponsive gel film.

Four swelled sheets of gel films (100 x 90 mm^2) were immersed in water and their total volume was adjusted to 30 cm^3 with pure water. Acetaldehyde (90% solution, 150 μL) and 1 mol L^{-1} hydrochloric acid (600 μL) were added and reacted for 24 h at room temperature to obtain thermoresponsive gel films. Prepared films were washed in pure water to remove unreacted chemicals. The size of films in response to temperature was measured in water at 5–50 °C.

3.3 Results and Discussion

Cationic hydrogels and anionic gel films were prepared by a cross-linking reaction of PVA in the presence of PDDA and PSS, respectively. Anionic gel films were dried before use. For adhesion of cationic hydrogels, an anionic dry-gel film was sandwiched between two pieces of cationic hydrogels. Anionic dry-gel films swelled with water uptake from two cationic hydrogels and adhered two hydrogels. The adhered gels remained adhered to each other over 1 week in water, but the two gels adhered to the swelled anionic hydrogel film were easily detached by immersing into water. These results indicate that the swelling of the anionic dry-gel film induced the adhesion between the cationic hydrogels. Interestingly, although adhered interfaces were optically transparent (**Fig. 3-2a**), wrinkle structures were observed at the adhered interface (**Fig. 3-2b**). When the anionic dry-gel film swelled in water, surface area of the film increased. Therefore, two cationic hydrogels adhered to each other with wrinkle formation by utilizing a swellable anionic dry-gel film. Since nonionic or anionic gels could not be adhered to, electrostatic interaction seems to be important as a foothold for wrinkle formation. To investigate the relationship between anionic film thickness and

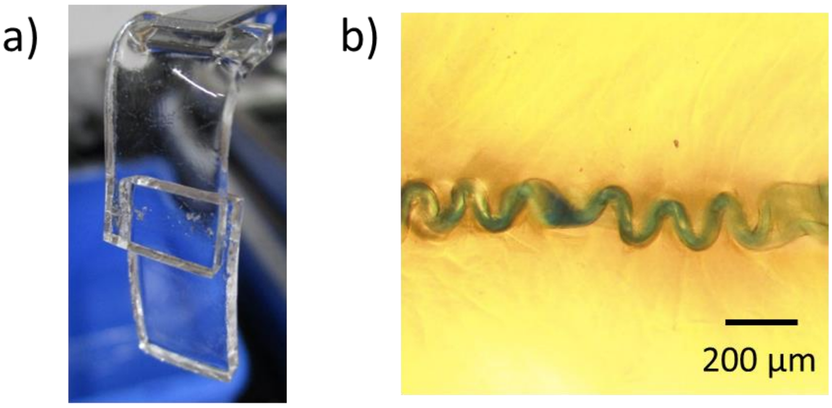

Fig. 3-2 (a) Preparation of PVA hydrogel by cross-linking reaction. (b and c) Chemical structure of (b) cationic PDDA and (c) anionic PSS.

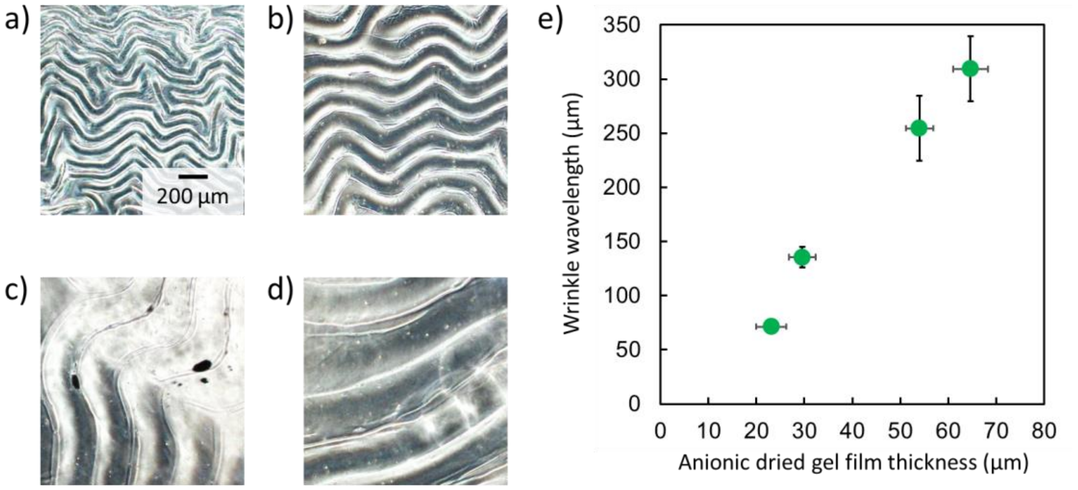

Fig. 3-3 (a-d) Phase-contrast microscopic observations of wrinkle structures at the interface of adhered hydrogels. The thickness of anionic dry-gel film was (a) 23±3, (b) 30±3, (c) 54±3, and (d) 64±4 µm, respectively. (e) Wrinkle wavelength as a function of anionic dry-gel film thickness.

wrinkle wavelength, anionic hydrogel films were prepared using different spacer thickness (50, 100, 150, and 200 µm). After immersing into ethanol and drying, the thickness of the anionic dried gel-films were measured using micrometer. Adhesion and wrinkle observation was performed with the same method. The relationship between the dried gel-film thickness and wrinkle wavelength is shown in **Fig. 3-3**. From this result, wrinkle wavelength was increased with increasing the anionic dry-gel film thickness. In order to clarify the origin of wrinkle formation during hydrogel adhesion, anionic dry-gel films were prepared with different shrinking ratios. During re-swelling at the interface of gels, the swelling ratio of these films would be different. To produce dry films with different swelling ratios when immersed in water, ethanol-water mixture was used as pretreatment because water is a good solvent but ethanol is a poor solvent for PVA. The mixture ratio of ethanol to water was changed from 100:0 to 0:100 v/v, and gel films which reached equilibrium swelled state in those solvents were dried on glass substrates. Each dry film was immersed in water and the swelling ratio was evaluated (**Fig. 3-4a**).

The increasing ratio in surface area in water was defined as A/A_0 ratio, where A and A_0 indicate areas of gel film after and before re-swelling in water, respectively. As shown in **Fig. 3-4b and c**, after immersing them into water, areas of all anionic gel films increased. A/A_0 ratio of anionic films upon re-swelling increases as films shrink significantly with increasing ethanol concentration during immersing because dry-gel films absorbed water by immersing into water and then they recovered their original size. Therefore, the A/A_0 ratio of the gel film varied depending on the ethanol-water ratio when the film was shrunk as a pretreatment.

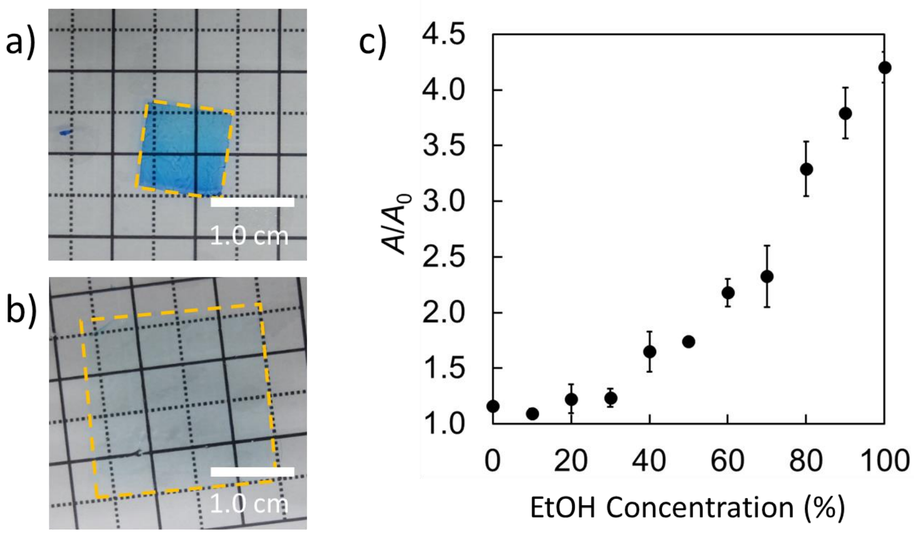

Fig. 3-4 (a,b) Macroscopic observations of swelled anionic gel films. EtOH concentrations during shrinkage as pretreatment were (a) 0 and (b) 80%, respectively. Initial size of each dried film was 1.0 x 1.0 cm^2. (c) A/A_0 ratio of anionic gel films as a function of EtOH concentration during shrinkage.

The cationic hydrogels were adhered to all anionic dry-films with different A/A_0 ratios. In microscopic observations of adhered gel–gel interfaces, three kinds of interface structures were observed as shown in **Fig. 3-5a**. In cases of lower A/A_0 (A/A_0 <1.7), no structures were observed at the adhered interfaces of gels. However, crease and wrinkle structures were observed in cases of middle (=2.2) and higher (>3.0) A/A_0 values, respectively. Wang and Zhao reported that crease and wrinkle structures were formed

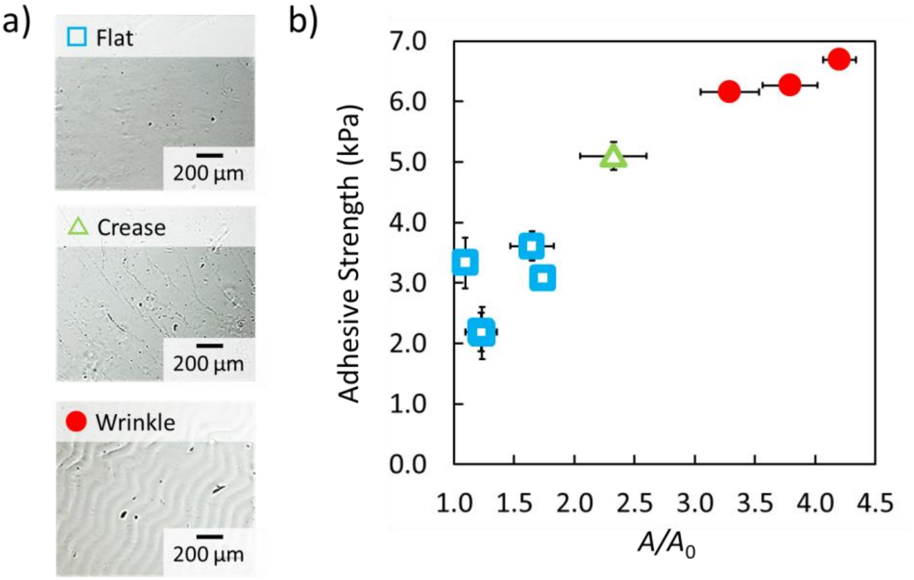

Fig. 3-5 (a) Phase-contrast observations of adhered interfaces of hydrogels with anionic films. (b) Adhesive strength of gels as a function of A/A_0 ratio of anionic dry gel films. Square, triangle, and circle symbols indicate that flat, crease, and wrinkle structures were formed at the adhered interfaces of gels. Closed symbols indicate gels were broken before detachment during tensile test.

under short and large strains of surface layer.[18] Wrinkle and crease structures formed at the adhered interfaces show similar tendencies. Thus, the formation of crease and wrinkle structures was induced by increasing area of the adhered gel films. Adhesive strength was measured to investigate the role of interface structures at adhesive interfaces. As shown in **Fig. 3-5b**, adhesive strength of no structure region ($A/A_0<1.7$) was weak and could be peeled off easily. Furthermore, there is no relationship between A/A_0 and adhesive strength. In the case of crease structure, adhesive strength was enhanced compared with flat interfaces. On the other hand, hydrogels with wrinkle structures ($A/A_0>3.0$) broke during the tensile test, indicating that the adhesion strength was sufficiently stronger than mechanical strength of the gels themselves. Usually, it is difficult to increase the area of the bonding interface, but hydrogel is a deformable elastic material. Therefore, the adhesive interface of the hydrogel was deformed by the swelling force caused by water uptake of the anionic dry gel film and formed a wrinkle structure. These results indicate that the surface area of the adhesion interface was obtained by wrinkle formation. Although it is conceivable that the adhesion strength is increased with increasing the surface area of adhesive interface, the formation of the wrinkle structure seems to play a role in further improving the adhesion strength of the hydrogel.

Next, hydrogels which adhered with aligned wrinkles were prepared and tensile tests in perpendicular and parallel directions were performed to investigate the role of wrinkle structures. The adhesive layer with oriented wrinkle structure was prepared by using anionic dry-gel film which swells to one direction (**Fig. 3-6a**). The anisotropic swelling films were prepared by shrinking the swollen film with both ends fixed in place during immersing into ethanol, then dried. The swelling of gel film caused the buckling of the adhered interface of hydrogels. It was expected that the wrinkling direction depended on the swelling direction of the gel film. In fact, oriented wrinkle structures were observed (**Fig. 3-6b and c**) in microscopic observation. The author performed tensile tests in perpendicular (**Fig. 3-6b**) and parallel (**Fig. 3-6c**) to the orientation direction of the wrinkles. From comparing the adhesion strength between these two types of aligned direction of wrinkles, it was noticed that the adhesion strength of parallel wrinkle structures was

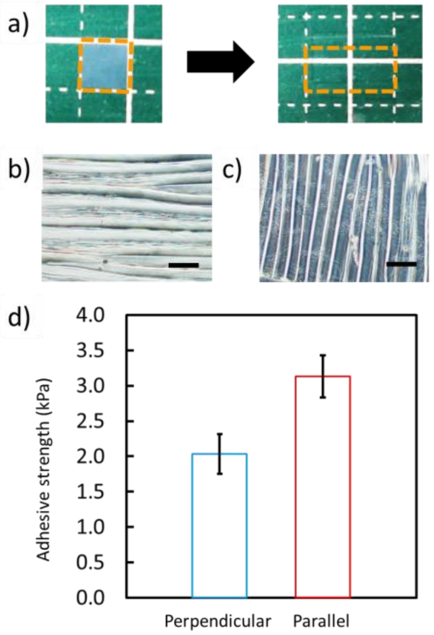

Fig. 3-6 (a) Swelling behavior of anisotropic swellable film. (b,c) Microscopic observation of adhered gel - gel interface with (b) perpendicular and (c) parallel orientation. (d) Adhesive strength of adhered gels with oriented wrinkle structures.

stronger than that with perpendicular structures (**Fig. 3-6d**). The difference in adhesive strength is explained by the deformation of wrinkle structures during tensile tests. The wavelength of parallel wrinkles was not changed when force was applied in the same direction for the orientation. However, perpendicular wrinkles were deformed due to straining during tensile test because the wrinkles were stretched in the wavelength direction. Therefore, it is suggested that deformation of wrinkles decrease the adhesion strength. As shown in **Fig. 3-7a**, the strongly adhered gels detached from each other cleanly by pulling the end of the film and stretching the wrinkles slowly. During film peeling, wrinkle structures were deformed from picked side to another side (**Fig. 3-7b**). After detachment, no damage was optically observed at the surfaces of detached cationic hydrogels (**Fig. 3-7c**). This result means that the adhesive strength was drastically decreased by deformation of wrinkle structures, indicating that wrinkle structures at the adhesive interface have the function to strengthen weak interactions between two pieces of materials. Conversely, when the polyelectrolyte concentration was increased to 50 mmol L^{-1}, the electrostatic interaction was too strong to deform the wrinkle, and the

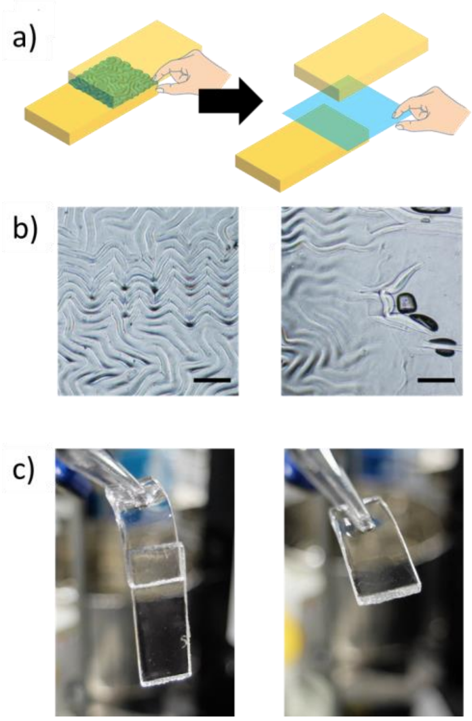

Fig. 3-7 (a) Experimental procedure of detachment of adhered gels by peeling of wrinkled film. (b) Microscopic observations of the wrinkled film in the hydrogel detachment test before (left) and during peeling (right). (c) Macroscopic observations of detachment of adhered gels by peeling wrinkling film. Before (left) and after (right) detachment test. Ionic monomer unit concentration and the cross-linking ratio of gels were 30 mmol L^{-1} and 0.5%, respectively. All scale bars indicate 200 μm.

adhered gel could not be detached. Therefore, the control of formation and deformation of wrinkle structures at the adhered interface of gels induced a strong adhesion and easy detachment of hydrogels.

Finally, it was demonstrate that adhesion control utilizing thermoresponsive gel-film (**Fig. 3-8a**), which prepared by reaction of PVA gels with acetaldehyde in acidic condition.[19] Present thermoresponsive gel-film shows lower critical solution temperature (LCST) type volume change, then they swelled in cool water but showed deswelling at hot water (**Fig. 3-8b and c**). The LCST could be modulated by changing the acetaldehyde concentration. When the thermoresponsive gel film which shrunk in hot water was sandwiched between two pieces of cationic hydrogels, hydrogels were adhered with wrinkle formation after cooling. The adhered interface was stable without detachment after immersing into water at 20 °C. Although the hydrophilicity and hydrophobicity of the surface of the thermoresponsive gel-film will change, the gel did not adhere without wrinkle formation. When temperature was increased to 50 ºC, wrinkle deformation was observed by phase-contrast microscopy (**Fig. 3-8d**). Then, the adhered gels detached immediately after immersing into water at 50 ºC (**Fig. 3-8e**) by deformation of wrinkle structure because the size of gel film decreased with water release. Thus, adhesion control was performed with wrinkle structure for hydrogels by using stimuli-responsive adhesive layer.

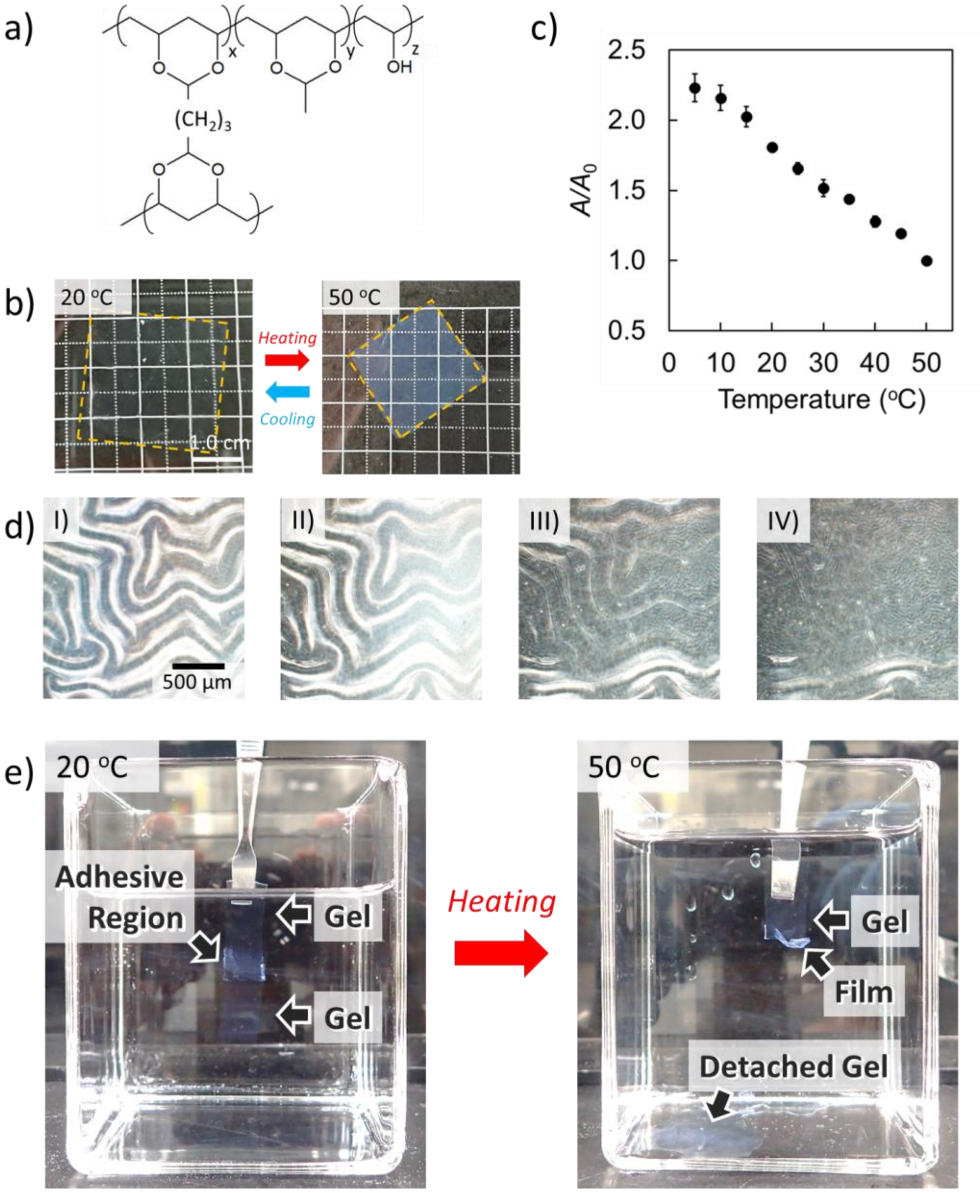

Fig. 3-8 (a) Chemical structure of thermoresponsive PVA film. (b) Macroscopic observations of thermoresponsive gel film at 20 and 50 °C in water. (c) A/A_0 ratio of thermoresponsive gel film as a function of temperature. d) Phase-contrast microscopic observations of adhered gel–gel interface. Observations were performed at 50 °C. Heating times were (I) 0, (II) 1, (III) 2, and (IV) 3 min, respectively. Initial temperature of adhered hydrogels was 20 °C. Ionic monomer unit concentration and the cross-linking ratio of gels were 50 mmol L^{-1} and 0.5%, respectively. Scale bar indicates 500 µm. e) Observations of adhered hydrogels immersed in water at 20 and 50 °C.

3.4 Conclusion

In conclusion, adhesion control for hydrogels was demonstrated utilizing wrinkling films. Wrinkle structures at the interface of adhered cationic hydrogels were formed by swelling of anionic dry-gel film used as the adhesive layer. Interface structures could be modulated by regulation of the swelling ratio of gel films, and adhesive strength of hydrogels was increased by formation of interface structures such as crease and wrinkle. Aligned wrinkle structures were formed by using an anisotropic swellable gel film. From the adhesion test for aligned wrinkled interfaces, it was found that the deformation of wrinkle structure decreased the adhesive strength of hydrogels. Therefore, adhered gels were detached without damage at their surface after peeling of wrinkled gel film. By using thermoresponsive gel films, the adhesion of hydrogels was controlled by wrinkle formation and deformation in response to temperature. Because both strong adhesion and easy detachment of hydrogels was perfomed utilizing stimuli-responsive wrinkle structures at adhesive interfaces, the presently wrinkled adhesive interface will be useful as a novel platform for the selective manipulation of microscale soft objects.

3.5 References

1. H. Lee, N. F. Scherer, P. B. Messersmith. *Proc. Natl. Acad. Sci. U. S. A.* **2006**, *103*, 12999-13003.
2. K. Zhan, C. Kim, K. Sung, H. Ejima, N. Yoshie. *Biomacromolecules* **2017**, *18*, 2959-2966.
3. A. Li, Y. Mu, W. Jiang, X. Wan. *Chem. Commun.* **2015**, *51*, 9117-9120.
4. L. Fang, L. Chang, W. Guo, Y. Chen, Z. Wang. *Appl. Surf. Sci.* **2014**, *288*, 682-689.
5. K. Autumn, Y. A. Liang, S. T. Hsieh, W. Zesch, W. Chan, T. W. Kenny, R. Fearing, R. J. Full. *Nature* **2000**, *405*, 681-685.
6. K. Autumn, M. Sitti, Y. A. Liang, A. M. Peattie, W. R. Hansen, S. Sponberg, T. W. Kenny, R. Fearing, J. N. Israelachvili, R. J. Full. *Proc. Natl. Acad. Sci. U. S. A.* **2002**, *99*, 12252-12256.
7. J. Duan, W. Xie, P. Yang, J. Li, G. Xue. Q. Chen, B. Yu, R. Liu, J. Zhou. *Nano Energy* **2018**, *48,* 569-574.
8. C. K. Roy, H. L. Guo, T. L. Sun, A. B. Ihsan, T. Kurokawa, M. Takahata, T. Nonoyama, T. Nakajima, J. P. Gong. *Adv. Mater.* **2015**, *27*, 7344-7348.
9. T. Nakamura, Y. Takashima, A. Hashidzume, H. Yamaguchi, A. Harada. *Nat. Commun.* **2014**, *5*, 4622.
10. Y. Kobayashi, Y. Takashima, A. Hashidzume, H. Yamaguchi, A. Harada. *Sci. Rep.* **2013**, *3*, 1243.
11. T. Asoh, H. Yoshitake, Y. Takano, A. Kikuchi. *Macromol. Chem. Phys.* **2013**, *214*, 2534-2539.
12. M. Kato, Y. Tsuboi, A. Kikuchi, T. Asoh, *J. Phys. Chem. B* **2016**, *120*, 5042-5046.

13. D. Martina, C. Creton, P. Damman, M. Jeusette, A. Lindner. *Soft Matter* **2012**, *8*, 5350-5357.
14. M. Kato, T. Asoh, H. Uyama. *Chem. Commun.* **2019**, *55*, 4170-4173.
15. X. Lei, D. Ye, J. Chen, S. Tang, P. Sun, L. Chen, A. Lu, Y. Du, L. Zhang. *Chem. Mater.* **2019**, *in press*. DOI: 10.1021/acs.chemmater.9b02812
16. H. Lee, D. Um, Y. Lee, S. Lim, H. Kim, H. Ko, *Adv. Mater.* **2016**, *28*, 7457-7465.
17. P. Rao, T. Sun, L. Chen, R. Takahashi, G. Shinohara, H. Guo, D. R. King, T. Kurokawa, J. Gong. *Adv. Mater.* **2018**, *30*, 1801884.
18. Q. Wang, X. Zhao. *Sci. Rep.* **2015**, *5*, 8887.
19. D. Christova, S. Ivanova, G. Ivanova. *Polym. Bull.* **2003**, *50*, 367-372.

Concluding Remarks

In this doctoral thesis, stimuli-responsive wrinkles were fabricated at the interfaces of hydrogels, and their function in adhesion was investigated.

In Chapter 1, a novel wrinkle structure formation method for hydrogel surface was developed using electrophoresis. Wrinkle structures were fabricated by PIC formation at the surface of hydrogels. It was found that the origin of wrinkle formation was stress-mismatch between PIC as a hard thin layer and hydrogel as a substrate, and the wavelength of wrinkle structures was controllable by changing the electrophoresis conditions such as applied electric field intensity and Young's modulus of hydrogels. The patterned and gradient wrinkle structures were fabricated by electrode modulating. Aligned wrinkles (herringbone and straight structures) to the direction of stretching, were fabricated on the surface of uniaxially stretched hydrogels after electric field impression. After unloading, hierarchical wrinkle structures were fabricated because new aligned wrinkles appeared in the perpendicular direction to the stretching, owing to the stress-mismatch between PIC and hydrogel. Wrinkles fabricated at the surface of thermoresponsive hydrogels can switch their geometrical configurations upon heating, which is triggered by the jumping of Young's modulus at specific temperature.

In Chapter 2, wrinkle structures were fabricated at adhered hydrogel interfaces using electrophoresis, and their function in adhesion was investigated. For the strong adhesion with wrinkle formation at adhered interfaces, spatial control of hydrogel networks such as density, distribution, and mobility of interactive units was important. The wavelength of wrinkles at the adhered hydrogel interfaces was controllable by

Young's modulus of gels. Thus, the wrinkle structure at adhesive hydrogel interfaces was formed by the elasticity mismatch of hydrogels and PIC layers. Increasing the compression ratio of hydrogels resulted in a decrease in the adhesive strength along with wrinkle disappearance. Therefore, it was considered that wrinkle structure at the adhered interface of hydrogels has a great impact on the adhesive strength of hydogels.

In Chapter 3, adhesion control for hydrogels utilizing wrinkle structures was demonstrated. Wrinkle structures at the interface of adhered cationic hydrogels were formed by swelling of anionic gel film used as the adhesive layer. Interface structures could be modulated by regulation of the swelling ratio of gel films. With increasing the swelling ratio of gel film as adhesive layer, adhesive strength of hydrogels was increased, and interface structures such as creases and wrinkles were formed. Aligned wrinkle structures were formed by using an anisotropic swellable gel film. The lap-shear adhesive strength with wrinkles aligned to the direction of tensile direction was higher than that aligned to the perpendicular direction. Thus, adhesive strength was decreased by wrinkle deformation during tensile test. Adhered gels were detached without damage at their surface after peeling of wrinkled gel film. By using thermoresponsive gel films, efficient adhesion control of hydrogel was achieved by utilizing the formation and deformation of wrinkle structure in response to the temperature.

The technique developed in this thesis extends the scope of the usage of wrinkle structures at hydrogel interfaces and gives impact on the development in a number of fields such as platform which attach materials containing water. The author believes the technology marked here will open a new avenue of hydrogel wrinkles and contribute to the next-generation functional surfaces.

List of Publications

1. Hydrogel Adhesion with Wrinkle Formation by Spatial Control of Polymer Networks.

   Masatoshi Kato, Yasuyuki Tsuboi, Akihiko Kikuchi, Taka-Aki Asoh

   J. Phys. Chem. B **2016**, *120*, 5042-5046.

2. Electrophoretic Fabrication of an Active and Selective Wrinkle Surface on Hydrogels.

   Masatoshi Kato, Taka-Aki Asoh, Hiroshi Uyama

   Chem. Commun. **2019**, *55*, 4170-4173.

3. Hydrogel Adhesion by Wrinkling Films.

   Masatoshi Kato, Taka-Aki Asoh, Hiroshi Uyama

   Macromol. Rapid Commun. **2019**, *40*, 1900434 (1-6).

4. Geometry Control of Wrinkle Structures Aligned on Hydrogel Surfaces.

   Masatoshi Kato, Taka-Aki Asoh, Hiroshi Uyama

   Langmuir **2020**, *in press* (DOI: 10.1021/acs.langmuir.9b03967a).

Acknowledgments

This study was performed at the Department of Applied Chemistry, Graduate School of Engineering, Osaka University, from 2017 to 2020.

First of all, I would like to thank my supervisor, Prof. Hiroshi Uyama, for his continuous guidance, invaluable discussion and kindhearted encouragement throughout this work. Without his encouragement, this dissertation would not have materialized. I sincerely thank him for providing me with great deals of chance to acquire new experiences. Precious experiences that I have absorbed will guide my future.

I am profoundly grateful to Prof. Akinori Saeki and Prof. Takahiro Kozawa for their valuable comments and suggestions on preparation of this thesis.

I also sincerely thank to Associate Prof. Taka-Aki Asoh. He gave me great chances not only research, but also many conferences. He gave me insightful comments and suggestions to every challenge I have faced throughout this study. Without his wisdom, this thesis would not have been possible.

I owe my deepest gratitude to Prof. Yasuyuki Tsuboi and Senior Lecturer Tatsuya Shoji (Graduate School of Science, Osaka City University) for their helpful discussions in my master degree, and continuous encouragement and support to pursue my doctoral degree.

I also appreciate the kind support and valuable help from Prof. Akihiko Kikuchi and Assistant Prof. Syuuhei Komatsu (Graduate School of Industrial Scienece and Technology, Tokyo University of Science).

I deeply thank Associate Professor Takashi Tsujimoto (Department of Natural and Environmental Science, TEIKYO University of Science) for his kind and valuable advices and support.

I wish to express my sincere thanks to Assistant Prof. Yu-I Hsu, Dr. Xinnan Cui and Dr. Yasushi Takeuchi for their expert advises and kind help.

My appreciation goes also to the previous and current fellow in the lab: Dr. Yu Shu, Dr. Tomonari Kanno, Dr. Qidong Wang, Ms. Zhaohang Wang, Mr. Chen Qian, Mr. Zhengtian Xie, Ms. Yankun Jia, Mr. Toshiki Tamiya, Mr. Shunsuke Mizuno, Mr. Naharullah bin Jamaluddin, Mr. Raghav Soni, Ms. Hanyu Wen, Ms. Yanting LYU, Mr. Akihide Sugawara, Mr. Mark Adam Malaluan Ferry, Ms. Yan Wang, Mr. Luwei Zhang, Ms. Meng Wei, Ms. Jiaxin Chen, Mr. Ginga Hoshi, Mr. Toshiki Honda, Mr. Tatsuya Yamamoto, Ms. Anna Shigaki, Mr. Yuxiang Jia, Mr. Yuya Fujiwara, Ms. Shiho Takai, Ms. Airi Ozaki, Ms. Madhurangika Panchabashini Horathal Pedige, Ms. Kotoha Fukushima, Ms. Yuuka Kashihara, Mr. Kohei Kikkawa, Mr. Yuki Shioji etc. for their kind help, assistance and friendship. And I also deeply appreciate the kind help and warm-hearted support from Ms. Yoko Uenishi, Ms. Tomoko Shimizu, Ms. Kyoko Tanimura, Ms. Chiaki Yoshizawa, Ms. Akiko Nakano, Ms. Yoshimi Shinomiya, Ms. Fumie Kamada and Ms. Mie Iwamoto.

I am also grateful to the Japan Society for the Promotion off Science (JSPS) for providing a doctoral scholarship. This study financially supported by a Grant-in-Aid for Scientific Research from JSPS (Grant Number: 18J10396)

Finally, I would like to extend my appreciation to my family for their endless love, support and understanding.

January 2020

Masatoshi Kato